PLEASE NOTE:

In all cases this material has been filmed in the best possible way from the available copy. Problems encountered with this document have been identified here with a check mark ✓.

1. Glossy photographs _____
2. Colored illustrations _____
3. Photographs with dark background _____
4. Illustrations are poor copy _____
5. Print shows through as there is text on both sides of page _____
6. Indistinct, broken or small print on several pages _____ throughout _____
7. Tightly bound copy with print lost in spine _____
8. Computer printout pages with indistinct print ✓
9. Page(s) _____ lacking when material received, and not available from school or author _____
10. Page(s) _____ seem to be missing in numbering only as text follows _____
11. Poor carbon copy _____
12. Not original copy, several pages with blurred type _____
13. Appendix pages are poor copy _____
14. Original copy with light type _____
15. Curling and wrinkled pages _____
16. Other _____

University Microfilms International

300 N. ZEEB RD., ANN ARBOR, MI 48106 (313) 761-4700

THE UNIVERSITY OF OKLAHOMA

GRADUATE COLLEGE

THEORY OF ELECTRON-PHOTON COINCIDENCE MEASUREMENTS IN ELECTRON-MOLECULE SCATTERING

A DISSERTATION

SUBMITTED TO THE GRADUATE FACULTY

in partial fulfillment of the requirements for the

degree of

DOCTOR OF PHILOSOPHY

BY

JAMES EVERETT POTTER

Norman, Oklahoma

1978

THEORY OF ELECTRON-PHOTON COINCIDENCE MEASUREMENTS IN ELECTRON-MOLECULE SCATTERING

A DISSERTATION

APPROVED FOR THE DEPARTMENT OF PHYSICS AND ASTRONOMY

BY

Roger Freund

J. M. Wadehra

David E. Golden

David Bruce

Michael A. Morrison

S. E. Babb, Jr.

ACKNOWLEDGEMENTS

I wish to express my deep appreciation to Dr. J. N. Huffaker for his help and guidance in directing this thesis, to Dr. D. E. Golden for suggesting this problem and for helpful discussions throughout the work, and to Dr. Michael Morrison for many interesting and instructive discussions of atomic and molecular physics. I also wish to thank the other members of my committee, Dr. S. E. Babb, Dr. David Branch, and Dr. Roger Frech for reading the thesis and to express my gratitude to all of the above for being on my committee.

TABLE OF CONTENTS

LIST OF TABLES

LIST OF ILLUSTRATIONS

ABSTRACT

Equations for the coincidence rate of electron-photon detection in electron-molecule scattering are derived in terms of the excitation amplitudes for the magnetic sublevels of rotational states of diatomic molecules. Applications to some electronic states of H_2 are discussed. Experimental feasibility is considered, and effects of relaxing assumptions are discussed.

CHAPTER I

INTRODUCTION

Scattering processes have been used to study atoms and molecules since the advent of modern physics. In this study, theory and experiment have played their usual complementary roles: as experimental techniques improved, more detailed theories were developed to explain the observations; and, conversely, more sophisticated theories required new and more accurate measurements for their verification.

The focus of the present work is on inelastic electron scattering from atoms or molecules, followed by photon emission from the atom or molecule. Recently, delayed coincidence techniques, long used to study nuclear collisions,[1] have been applied to this type of scattering. Delayed coincidence, as used in this context, refers to detection of the photon a certain (measured) time interval after the occurrence of the scattering event. A variety of different kinds of delayed coincidence experiments are possible. The ideal one would be a spin-polarized, mono-energetic beam incident on targets with all quantum numbers known. The momentum vector and spin of the scattered electron, as well as the time delay, energy, polarization, and direction of the emitted photon would be measured. The complete analysis of such an experiment (also

borrowed from nuclear physics[2,3]) would provide information about the scattering process and the excited states: in addition to mean lifetimes and differential cross sections, one could determine orientation and alignment parameters and the relative phases of excitation amplitudes to different magnetic sublevels.

Several reviews of experimental and theoretical developments of coincidence measurements in electron scattering from atoms and molecules have been published.[4-6] Following is a brief summary of these developments, beginning with atomic scattering.

A. Types of Electron-Atom Coincidence Measurements and Theory

1. Lifetimes.

The simplest coincidence experiment is one used to determine the lifetimes of excited atomic states. The first measurements of this type were reported by Heron et.al. in 1954.[7,8] Their method was to detect photons resulting from the decay of excited states of helium in coincidence with the pulsed electron beam used to produce the excited states.

The accuracy of atomic lifetime measurements was significantly increased by Imhoff and Read in 1969.[9] Their technique was to detect a photon and the single electron that had excited the state in coincidence.

By measuring the energy-loss of the electron, they were able to eliminate the effect of cascades into the state.

2. Differential Cross Sections.

If the direction of the scattered electron is observed, the differential cross section can be determined. Ehrhardt et. al.[10] found differential ionization cross sections of helium by measuring angular correlations between the scattered and emitted electrons. The absolute differential cross sections for electron excitation of the 4'S, 4'D, 5'S, and 5'D states of helium were measured by Pochat et. al.[11] utilizing a coincidence technique. This experiment demonstrated an advantage of the coincidence technique for finding cross sections: because the states listed above were not resolvable using an electron spectrometer, the higher resolution possible in the photon detector was used to select a particular state.

3. Polarization.

A theoretical analysis of the polarization of the radiation from electron impact excitation was given by Percival and Seaton,[12] who related the polarization to the cross sections for exciting magnetic substates of the atom. Measurements of the polarization using electron-photon coincidence were made by King et. al.[13] who detected only electrons scattered in the forward direction.

4. Angular Correlation.

The measurement of angular correlations in addition to the polarization and time delay may provide information on lifetimes, differential cross sections, fine and hyperfine split-

tings, orientation and alignment parameters, and complex excitation amplitudes. The theoretical analysis was made by Macek[14,15] and Macek and Jaecks[16] in 1971. This work will be discussed further in Chapter II. Several other theoretical papers followed, among them Wykes,[17] Jacobs,[18] and Fano and Macek.[19] The latter work is a more abstract reformulation of Ref. (16), emphasizing orientation and alignment parameters. A density matrix[20] approach to this problem was used by Blum and Kleinpoppen[21,22] and by Eichler and Fritsch.[23]

The first measurements of angular correlations were reported by Eminyan, MacAdam, Slevin, and Kleinpoppen,[24,25] using helium as the target gas. Other important measurements of angular correlations were made by Arriola et. al.[26] (but see Slevin and Farago[27] for a criticism of this work), Ugbabe et. al.[28] and Sutcliffe et. al.[29]

The angular correlation measurements stimulated theoretical calculations of cross sections for exciting the magnetic substates of the atoms as well as calculations of the relative phases between excitation amplitudes. These calculations were carried out using several different methods:

i.) distorted wave,[30]

ii.) first order many-body (random phase),[31]

iii.) eikonal,[32]

iv.) close coupling,[33] and

v.) distorted wave, polarized orbital.[34]

B. Types of Molecule-Electron Coincidence Measurements and Theory

1. Lifetimes.

Coincidence techniques have been used quite effectively in determining accurate lifetimes for molecular states. The first electron-photon coincidence measurements of molecular lifetimes were made by Imhoff and Read in 1971.[35] As in the atomic case, the detection of the electron is used to fix the time of formation of the excited state and the time delayed detection of the photon is used to find the lifetime. This was extended[36] to lifetimes of ionic states for the process

$$e + M \rightarrow M^{*+} + e_1 + e_2$$

$$M^{*+} \rightarrow M^{+} + \gamma \ .$$

It can be shown that either e_1 or e_2 usually has almost all the excitation energy, thus the detection of <u>one</u> of these electrons serves the same purpose as the electron in the previous example.

Backx, Kleiver, and VanderWeil[37] measured the lifetime of the $B^2\Sigma$ state of CO^+ with a triple coincidence: the scattered electron, the decay photon, and the CO^+ ion.

Radiative lifetime measurements of simple free radicals (NH and CH) formed in the electron impact dissociation of parent molecules (NH_3 and CH_4) utilizing an electron-photon coincidence[38] were reported in 1978.

2. Polarization.

The work of Percival and Seaton[12] was extended to diatomic molecules by Jette and Cahill[39] and in the united-atom and Born approximations by Baltayan and Nedelec.[40] These works are not satisfactory for analysis of coincidence measurements because they are time-independent; Ref. (39) is limited to threshold excitation.

3. Differential Cross Sections.

Few measurements have been made of molecular differential cross sections with coincidence methods. Böse[41] has reported electron impact ionization cross sections for D_2 using a photon-photon coincidence method for the process

$$e + D_2 \rightarrow 2e' + D_2^{**} \rightarrow \begin{matrix} D_{(2p)} \\ \downarrow \\ D_{(1s)}+\gamma \end{matrix} + \begin{matrix} D_{(2p)} \\ \downarrow \\ D_{(1s)}+\gamma \end{matrix}$$

and Böse and Linder[42] have performed an electron-photon coincidence measurement for ionization cross sections of D_2.

4. Angular Correlations.

Angular correlation measurements of electron-molecule scattering should provide the same type of information as that discussed in the atomic case. As yet, no such measurements have been reported. Only one theoretical paper has been published for the analysis of such an experiment: that by Blum and Jakubowicz.[43] Their paper uses the density matrix

approach, and results are formulated in terms of the Stokes parameters.

The purpose of the present work is to develop a theory of angular correlations between electrons and photons in electron-diatomic molecule scattering. It is an extension of the work by Macek and Jaecks[16] from atoms to diatomic molecules. The results are expressed in a form such that the coincidence rate is a linear combination of the complex excitation amplitudes. These complex excitation amplitudes may be uniquely determined when sufficient measurements are performed. Results are presented in a form suitable for analysis of experiments with or without measurements of the photon's polarization.

C. A Plan of This Work

The theoretical background of this research is reviewed in Chapter II. An examination of appropriate details of the formal theory of scattering as needed for this problem is followed by a detailed discussion of the theory of Macek and Jaecks[16] on which this work is closely modeled. The formal theory for analysis of angular correlation measurements of electron-diatomic molecule scattering is presented in Chapter III. Applications of this theory to some states of H_2 are made in Chapter IV, and the feasibility of such an experiment is discussed as well. In Chapter V, the theory is extended to the case where hyperfine structure may be important, and

effects of relaxing some of the assumptions of Chapter III are considered. Chapter VI contains a summary and conclusions. Appendix I is a summary of angular momentum theory and a brief review of the diagrammatic technique of Yutsis.[44] Two reductions of complicated expressions using this technique are presented in Appendix II. A Basic program for evaluating 3j and 6j coefficients is presented in Appendix III.

CHAPTER II

PRELIMINARIES

The scattering process under consideration in this work is molecular excitation via inelastic electron scattering,

$$e + M \rightarrow e' + M^{**} , \tag{2.1}$$

followed by photon emission,

$$M^{**} \rightarrow M^{*} + h\nu . \tag{2.2}$$

Here e and e' are the incident and scattered electron states, and M, M**, and M* are the initial, intermediate, and final states of the target diatomic molecule. We only consider the case where the scattered electron and the photon $h\nu$ are detected in coincidence.

The analysis of this process, presented in the following chapter, utilizes concepts from several areas of theoretical physics. Some necessary concepts are outlined in section A of this chapter: First, the complex excitation amplitude is defined. Its significance in this work is discussed, as well as its relation to the T matrix. Second, some elements of the theory of angular momentum are outlined. Third, the concept of coherent excitation is defined and discussed in the context of molecular states.

The theory of electron-atom coincidence measurements

as presented by Macek and Jaecks[14] is discussed in section B of this chapter.

A. Theoretical Foundations

1. Complex Excitation Amplitudes.

The usual situation in a scattering experiment is that the source of incident particles and the detectors are far from the interaction region. This means that observed quantities are related to the asymtotic wavefunction of the system, which therefore contains all the information that can be obtained from the scattering measurement.

The asymtotic form for an electron scattering inelasticly from an atom or molecule is[45]

$$\Psi_i^+(\vec{r},\eta) = \Phi_i(\vec{r},\eta) + \sum_f F_{fi}\phi_f(\eta)\frac{e^{ip_f r}}{r} \qquad (2.3)$$

where $\vec{r}$ is the scattered electron coordinate, $\Phi_i(\vec{r},\eta)$ is the initial state of the system given by

$$\Phi_i = \phi_0(\eta)e^{i(\vec{p}_i\cdot\vec{r})} . \qquad (2.4)$$

The initial target state is ϕ_0 with internal quantum numbers η, while $\vec{p}_i$ is the momentum of the incident electron (usually taken along the z-axis). The sum over f is to be taken over all energetically allowed final states of the target, denoted by ϕ_f. The quantity F_{fi} is the complex excitation amplitude; that is, the probability amplitude for scattering from the state Φ_i to the state

$$\Phi_f = \phi_f(\eta)e^{i(\vec{p}_f\cdot\vec{r})} , \qquad (2.5)$$

where ϕ_f is the final state of the target and $\vec{p}_f$ is the scattered electron momentum vector. Finally, the excitation amplitude is given by

$$F_{fi} = - \frac{m_e}{2\pi\hbar^2} \langle \Phi_f | \hat{v} | \Psi_i^+ \rangle \tag{2.6}$$

with $\hat{v}$ the scattering potential operator. In general the complex excitation amplitude depends on the electron energy as well as the coordinate directions (θ,ϕ) of $\vec{p}_f$.

A primary objective of this work is to relate the observed coincidence rate to the excitation amplitudes.

The differential cross section, $(d\sigma_{fi}/d\Omega)(\theta,\phi)$, is related to the excitation amplitude by

$$\frac{d\sigma_{fi}}{d\Omega} = \frac{p_f}{p_i} |F_{fi}|^2 \tag{2.7}$$

Clearly more information is contained in the scattering amplitude than in the cross section, since the latter is proportional to the modulus squared of the former.

The T matrix, or transition matrix, has convenient symmetry properties, which make it useful for studying general properties of scattering processes. For example, the T matrix is Lorentz invariant; and because pure rotations are contained in Lorentz transformations, the T matrix is invariant to pure rotations up to a phase factor. The complex scattering amplitude is given in terms of the T matrix by

$$F_{fi} = - \frac{m_e}{2\pi(\hbar)^2} \langle \Phi_f | \hat{T} | \Phi_i \rangle \tag{2.8}$$

$$F_{fi} = \frac{-m_e}{2\pi(\hbar)^2} T_{fi} \tag{2.9}$$

where the elements of the T matrix are defined by

$$T_{fi} = \langle \Phi_f | \hat{T} | \Phi_i \rangle \ . \tag{2.10}$$

2. Coupling of Angular Momenta.[46]

Consider a system which has two angular moments, $\vec{J}_1$ and $\vec{J}_2$. If the sum of these angular moments is $\vec{J}$, a complete set of commuting operators needed to represent this system might include H, J_1^2, J_2^2, J^2, and J_z with eigenvalue equations

$$J^2|jm\rangle = j(j+1)|jm\rangle \tag{2.11}$$

and

$$J_z|jm\rangle = m|jm\rangle \ . \tag{2.12}$$

However, if the interaction between these angular momenta is such that the z components of $\vec{J}_1$ and $\vec{J}_2$ are conserved separately, it may be convenient to use a different set of commuting operators consisting of H, $\vec{J}_1^2$, $\vec{J}_2^2$, J_{1z} and J_{2z}. The eigenvalue equations for this basis are

$$\vec{J}_1^{\,2}|j_1 m_1 j_2 m_2\rangle = j_1(j_1+1)|j_1 m_1 j_2 m_2\rangle \ , \tag{2.13}$$

$$J_{1z}|j_1 m_1 j_2 m_2\rangle = m_1|j_1 m_1 j_2 m_2\rangle \ , \tag{2.14}$$

and similarly,

$$\vec{J}_2^{\,2}|j_1 m_1 j_2 m_2\rangle = j_2(j_2+1)|j_1 m_1 j_2 m_2\rangle \ , \tag{2.15}$$

$$J_{2z}|j_1 m_1 j_2 m_2\rangle = m_2|j_1 m_1 j_2 m_2\rangle \ , \tag{2.16}$$

where the product representation $|j_1m_1\rangle|j_2m_2\rangle$ is denoted by $|j_1m_1j_2m_2\rangle$.

The desirability of using one or the other of these representations depends partially on the interactions present. This is discussed further in section B of this chapter.

Changing from one representation to the other is accomplished by a unitary transformation:

$$|jm\rangle = \sum_{m_1m_2} \langle j_1m_1j_2m_2|j_1j_2jm\rangle|j_1m_1j_2m_2\rangle \tag{2.17}$$

and

$$|j_1m_1j_2m_2\rangle = \sum_{jm} \langle j_1m_1j_2m_2|j_1j_2jm\rangle|jm\rangle . \tag{2.18}$$

The coefficients in the above equations are called vector coupling or Clebsch-Gordan (CG) coefficients. These CG coefficients are employed in this work as well as the related, but more symmetric Wigner 3-j coefficient:

$$\begin{pmatrix} j_1 & j_2 & j_3 \\ m_1 & m_2 & -m_3 \end{pmatrix} = (-1)^{j_1-j_2+m_3}(2j_3+1)^{-1/2}\langle j_1m_1j_2m_2|j_1j_2j_3m_3\rangle . \tag{2.19}$$

Symmetry properties of the 3-j coefficients are given in Appendix I.

The coupling of three angular momenta may be expressed in the uncoupled representation $|j_1m_1\rangle|j_2m_2\rangle|j_3m_3\rangle$, as well as in a coupled representation $|jm\rangle$ where $\vec{j}_1+\vec{j}_2+\vec{j}_3 = \vec{j}$ analogous to the coupling of two angular momenta. There are several different ways in which the three angular momenta

can be added two at a time, which lead to mathematically distinct representations: If, for example, $|j_1 j_2 (j_{12}) j_3 jm\rangle$ and $|j_1 j_2 j_3 (j_{23}) jm\rangle$ are obtained by $\vec{j}_1+\vec{j}_2 = \vec{j}_{12}$, $\vec{j}_{12}+\vec{j}_3 = \vec{j}$; and $\vec{j}_2+\vec{j}_3 = \vec{j}_{23}$, $\vec{j}_1+\vec{j}_{23} = \vec{j}$, respectively, the two sets of basis sets are related by the linear transformation

$$|j_1 j_2 (j_{12}) j_3 jm\rangle = \sum_{j_{23}} |j_1 j_2 j_3 (j_{23}) jm\rangle \times \times [(2j_{12}+1)(2j_{23}+1)]^{1/2} W(j_1 j_2 j j_3; j_{12} j_{23}) \quad (2.20)$$

where $W(j_1 j_2 j j_3; j_{12} j_{23})$ is a Racah coefficient. Again, Racah coefficients are related to the more symmetric 6-j coefficients by

$$\begin{Bmatrix} j_1 & j_2 & j_{12} \\ j_3 & j & j_{23} \end{Bmatrix} = (-1)^{j_1+j_2+j_3+j} W(j_1 j_2 j j_3; j_{12} j_{23}) . \quad (2.21)$$

The symmetry properties of 6j coefficients are given in Appendix I.

3. Coherent Excitation.

One of the assumptions used in the present work involves the concept of coherent excitation of molecular levels. The purpose of this section is to clarify what is meant by coherent excitation in the context of molecular or atomic states.

The system of interest consists of an ensemble of diatomic molecules and a beam of monoenergetic incident electrons. The state of the incident electrons may be specified

by the momentum vector and spin orientation: $|\vec{p}_i, m\rangle$. Similarly, the scattered electron state is given by $|\vec{p}_f m\rangle$. The spin orientation is the same in both states if it is assumed that the scattering interaction has no spin dependent terms.

In an ensemble of diatomic molecules it may reasonably be expected that the quantum numbers Λ and S are known, but not the rotational quantum number K. (Here, Λ is the projection of the orbital electronic angular momentum onto the internuclear axis, and S is the total electron spin.) The state must then be described by a statistical mixture of the pure eigenstates. (The statistical weight of the various K states is determined by the Boltzmann distribution for the gas.)

One may think of the above ensemble of molecules as an ensemble of systems, each in some pure state. Now consider the excitation of one of these pure states. The linearity of the Schrodinger equation assures that immediately after the excitation the system is still in a pure state. This excited state, denoted by $|\psi\rangle$, is a superposition of all possible excited states of the system. Each excited state is the direct product of the molecular and electron kets. The quantum number K may be determined from detection of $h\nu$, so that $|\psi\rangle$ can be written as

$$|\psi\rangle = \sum_{M_K=K,K-1,\ldots,-K} [f_{M_K}(\vec{p}_i, \vec{p}_f)\,|KM_K\rangle|\vec{p}_f, m\rangle + \cdots \qquad (2.22)$$

where M_K is the z-projection of K, and $f_{M_K}(\vec{p}_i, \vec{p}_f)$ is the

complex excitation amplitude for exciting the M_K^{th} magnetic sublevel. All other known quantum numbers have been suppressed. The three dots indicate similar terms for all other accessible states ofthe system, including other values of K.

In the absence of an external field, the magnetic substates of K are energetically degenerate. This implies that the electrons scattered in a particular direction from all the M_K levels of a given K have the same momentum as well, so that $|p_f m>$ can be factored from the sum in Eq. (2.22):

$$|\psi> = [\sum_{M_K} f_{M_K} |KM_K>] |\vec{p}_f m> + \cdots . \tag{2.23}$$

Because the state $|\psi>$ can now be expressed as a linear superposition of states $|KM_K>$, the magnetic substates are said to be coherently excited, i.e., the kets have a fixed phase relationship.

In practice, the electron beam will not usually be monoenergetic, but will have some spread of energies, ΔE, around a central value, $\frac{p_i^2}{2m_e}$. When this situation holds, the scattered electron state may be factored from other levels that lie within $\Delta E/2$ of the K^{th} level of Eq. (2.23). Thus levels that are not exactly energetically degenerate may be coherently excited in the sense that

$$|\psi> = [\sum_K \sum_{M_K} f(KM_K) |KM_K>] |\vec{p}_f m\rangle + \cdots \tag{2.24}$$

where the sum includes all K such that

$$\frac{p_i^2 - p_f^2}{2m_e} - \frac{\Delta E}{2} \leq E_K \leq \frac{p_i^2 - p_f^2}{2} + \frac{\Delta E}{2} \tag{2.25}$$

and E_K is the excitation energy of the K^{th} level. Since $|\vec{p}_f|$ is not known precisely in this case, this expression implies that $|\vec{p}_f m\rangle$ includes all scattered electron states with the range $p_f \pm \sqrt{2\Delta E m_e}$, i.e., Eq. (2.24) must be integrated between these limits.

B. Discussion of Atomic Electron-Photon Coincidence Measurements

1. Introduction.

The work by Macek and Jaecks,[14] hereafter referred to as MJ, has been very useful in the analysis of coincidence experiments involving electron-atom scattering. Briefly, they present formulas which express coincidence rates in terms of complex excitation amplitudes, detector coordinates, photon polarization, and time resolution of the apparatus. These formulas may be readily used to determine cross sections or excitation amplitudes from measured rates. Since this theory is so useful, we decided to construct our electron-molecule scattering theory in close analogy with MJ. Because of the importance of the work of MJ and its close relationship to the present work, a summary of the theory is presented in the remainder of this chapter.

A few typographical errors occur in the original paper; we attempt to correct these in this discussion. Algebraic details common to both atomic and molecular cases, which are

not essential for understanding of the atomic case, are presented in the context of molecular scattering in the next chapter.

The scattering process treated by MJ is general in the sense that it can involve electrons, ions, atoms, molecules, or other breakup products. The only restriction is that the emitted radiation must come from an atom. The emphasis in this discussion is on electron-atom scattering. In particular, the process is represented schematically by

$$e + A \rightarrow e' + A^{**} , \tag{2.26}$$

followed by the photon decay,

$$A^{**} \rightarrow A^{*} + h\nu , \tag{2.27}$$

where initial, intermediate, and final atomic states are denoted by A, A**, and A*, respectively.

2. Assumptions of MJ.

The initial assumptions used in MJ are listed below:

i. The atom obeys LS coupling*.

ii. The duration of the collision is short compared to the mean lifetime of the excited state, permitting the excitation and decay processes to be treated separately.

---

*In LS coupling, the total orbital angular momentum, $\vec{L}$, is coupled to the total electronic spin, $\vec{S}$, to form the total electronic angular momentum, $\vec{J}$.

iii. Cascades from higher excited states have a negligible effect.

iv. The light detection system detects all radiation near the central frequency of a line, and the undetected wings do not contain significant radiation.

v. The decay of the excited state is an electric dipole transition.

vi. The scattering Hamiltonian has no spin-dependent terms.

vii. The spin-orbit coupling in the atom is neglected.

3. The Coincidence Rate Expression.

The coordinate system used in MJ (as well as the present work) is shown in Fig. 1. The primed and unprimed coordinates refer to the photon and electron detectors, respectively. The incident beam is along the z axis, which is also the quantization axis for projections of angular momenta. Because the directions of the photon and scattered electron are required in the coincidence formulas, the scattering region must be well-localized: either crossed beams for incident and target particles, or an incident beam and a thin target foil. Consistent with the discussion of coherent excitation in section B, the magnetic sublevels for given L are coherently excited. In this situation, the excited state wavefunction is written as

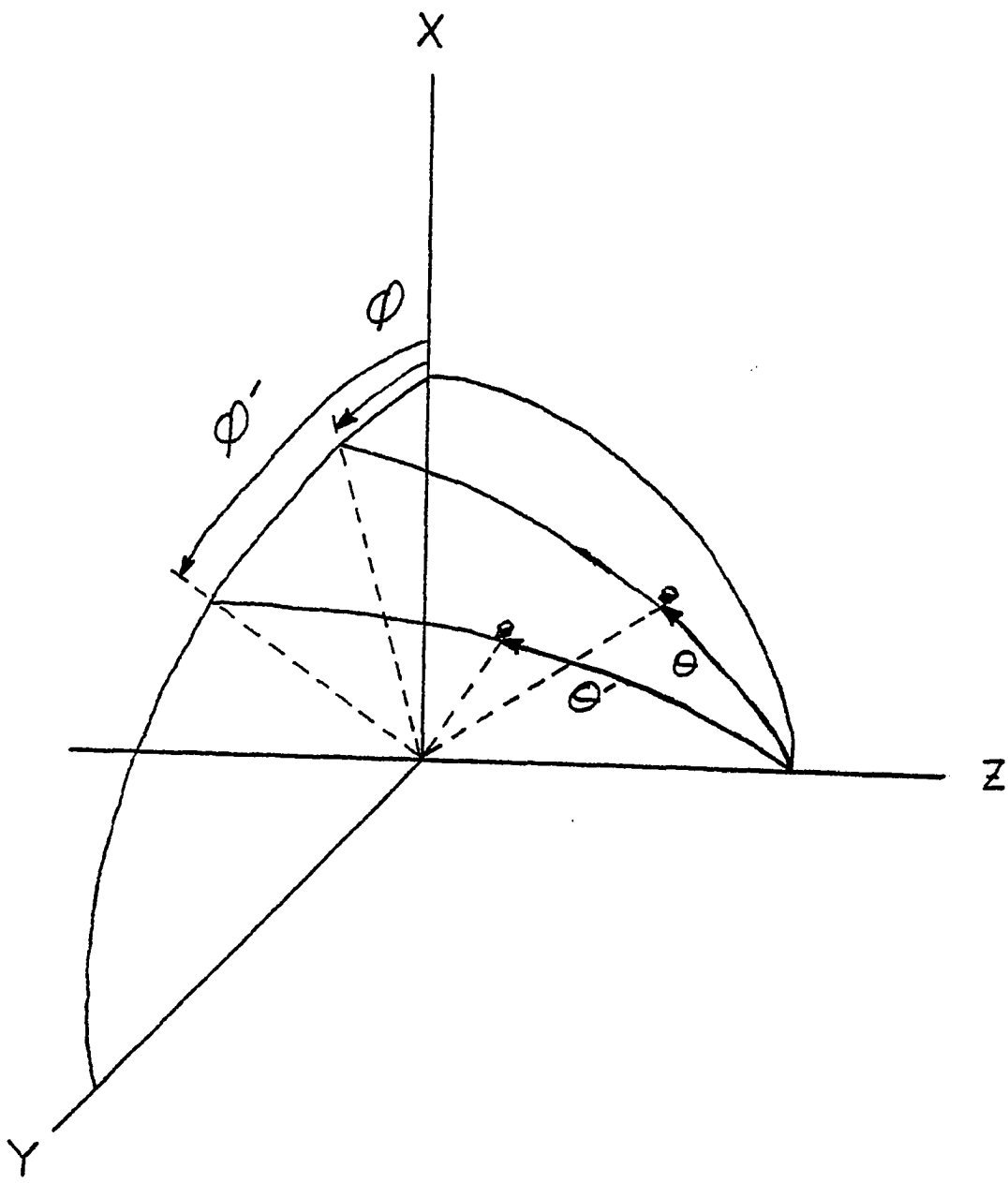

Fig. 1. Coordinate system used in MJ and in the present work. The primed coordinates refer to the photon detector and the unprimed coordinates refer to the electron detector. The electron beam is incident from the -Z direction.

$$|\psi> = \sum_{JFM_F} a(JFM_F)|JFM_F> e^{-(\frac{\gamma}{2} + i\frac{E_{JF}}{\hbar})t} . \qquad (2.28)$$

The quantities $a(JFM_F)$ are the complex excitation amplitudes for exciting the state $|JFM_F>$, $\frac{1}{\gamma}$ is the mean lifetime of the state, and t is the elapsed time after the excitation. The total angular momentum of the state is $\vec{F}$, where $\vec{F}=\vec{J}+\vec{I}$ and $\vec{I}$ is the nuclear spin of the atom. The imaginary term in the exponential is indicative of coherent excitation. It is responsible for the oscillation in total intensity of radiation as a function of time.

The coincidence rate is given by

$$\frac{dN}{d\Omega d\Omega'} = vn_0 n_A \frac{e^2\omega^3}{2\pi hc^3} \sum_0 \int_0^{\Delta t} dt |<0|\hat{\varepsilon}\cdot\vec{x}|\psi>|^2 . \qquad (2.29)$$

In this equation v is the electron speed, n_0 is the incident particle density, n_A is the target density, ω is the frequency of emitted radiation, 0 represents the final states for the decay, $\hat{\varepsilon}$ is the polarization vector of the radiation, $\vec{x}$ is the dipole length operator, and Δt is the resolution time of the apparatus, and $d\Omega$ and $d\Omega'$ are differential solid angles for the electron and photon directions, respectively. This equation shows that the coincidence rate per unit solid angle is proportional to the probability for decay integrated over the "on time" for the apparatus and summed over the unresolved final states of the atom. Any unknown quantum numbers of the initial state must be averaged over. For this case that means the electron and nuclear spin projec-

tions of the initial state must be averaged over.

The next objective is to reduce the number of parameters needed in the coincidence formula. This is accomplished in six steps:

i.) Substituting Eq. (2.28) into Eq. (2.29) with the vector operators written in spherical tensor components (q and q') gives

$$\frac{dN}{d\Omega d\Omega'} = vn_0 n_A \left(\frac{e^2\omega^3}{2\pi hc^3}\right) \sum a^*(J'F'M_F')a(JFM_F)$$

$$\times (-1)^{q+q'} \varepsilon_{-q'}^* \varepsilon_{-q} \langle L_0 M_{L_0} S_0 M_{S_0} I_0 M_{I_0} | X^1_{q'} | LS(J')IFM_F' \rangle^*$$

$$\langle L_0 M_{L_0} S_0 M_{S_0} I_0 M_{I_0} | X^1_q | LS(J)IFM_F \rangle \int_0^{\Delta t} dt\, e^{-(\gamma + i\omega_{JF,J'F'})t} \tag{2.30}$$

where

$$\omega_{JF,J'F'} \equiv \frac{E_{JF} - E_{J'F'}}{\hbar} , \tag{2.31}$$

and the sum is over q, q', J, F, M_F, J', F', M_F', M_{L_0}, M_{S_0}, and M_{I_0}. In this equation the ket $|JFM_F\rangle$ has been written with the coupling indicated explicitly as

$$|JFM_F\rangle \rightarrow |LS(J)IFM_F\rangle , \tag{2.32}$$

and likewise

$$|J'F'M_F'\rangle \rightarrow |LS(J')IF'M_F'\rangle . \tag{2.33}$$

ii.) The coupled basis is replaced by the uncoupled ba-

sis using the CG coefficients introduced earlier:

$$|LS(J)IFM_F> = \sum_{M_L M_S M_I M_J} |LM_L SM_S IM_I><LM_L SM_S|LSJM_J> \times$$

$$<JM_J IM_I|JIFM_F> \qquad (2.34)$$

and

$$a(JFM_F) = \sum_{M_L M_S M_I M_J} a(LM_L SM_S IM_I) \times$$

$$<LM_L SM_S|LSJM_J><JM_J IM_I|JIFM_F> . \qquad (2.35)$$

iii.) When the excitation amplitudes in Eq. (2.30) are replaced by those of Eq. (2.35), products like $a^*(LM_L'SM_S'IM_I)$ $a(LM_L SM_S IM_I)$ occur. These excitation amplitudes depend on both θ and ϕ. This ϕ dependence may be removed by taking advantage of the rotational invariance of $\hat{T}$, as discussed previously. The excitation amplitudes are proportional to elements of the T matrix so that

$$a^*(LM_L'SM_S'IM_I')a(LM_L SM_S IM_I) \propto$$

$$<\vec{p}_f LM_L'SM_S'IM_I'|\hat{T}|\vec{p}_i i>^* \times$$

$$<\vec{p}_f LM_L SM_S IM_I|\hat{T}|p_i i> , \qquad (2.36)$$

where $|i>$ denotes the initial state of the atom. Because of this proportionality, the excitation amplitudes have the same transformation properties as the T matrix elements. Now consider rotations about the z-axis of this product of matrix

elements. Eigenkets and eigenbras of angular momentum transform like

$$\hat{R}_{\hat{z}}(\phi)|jm\rangle = e^{im\phi}|jm\rangle \tag{2.37}$$

and

$$\langle jm|\hat{R}_{\hat{z}}(\phi) = e^{-im\phi}\langle jm| \tag{2.38}$$

Thus the phase factors from corresponding bras and kets in Eq. (2.36) cancel.

Assumption vi., that there are no spin-dependent terms in the scattering Hamiltonian, along with assumption vii., that the spin-orbit coupling is weak, together imply that

$$M_S = M_S' \tag{2.39}$$

and similarly,

$$M_I = M_I'. \tag{2.40}$$

Therefore the effect of this rotation on the product of amplitudes is

$$\hat{R}_{\hat{z}}(\phi)a^*(LM_L'SM_S'IM_I')a(LM_LSM_SIM_I)$$

$$= e^{i(M_L - M_L')\phi}a^*(LM'_LSM_S'IM_I')a(LM_LSM_SIM_I) \tag{2.41}$$

For an unpolarized beam and target, we must average over initial spin projections: this is accomplished by summing over projections and then dividing by the spin multiplicities. Including the ϕ-dependence explicitly, along with Eqs. (2.39) and (2.40), we can show the result of such averaging in the form

$$\int a^*(LM_L'SM_S'IM_I')a(LM_LSM_SIM_I) =$$

$$\frac{\delta_{M_IM_I'}\delta_{M_SM_S'}e^{i(M_L-M_L')\phi}}{(2S+1)(2I+1)} \langle a_{M_L'}, a_{M_L}\rangle \qquad (2.42)$$

where the amplitudes a_{M_L}, which depend only on θ, are normalized so that their modulus squared is the partial differential cross section for exciting the M_L^{th} magnetic sublevel:

$$|a_{M_L}|^2 = \frac{d\sigma_{M_L}}{d\Omega} . \qquad (2.43)$$

iv.) The fourth step involves use of the reflection symmetry in the scattering plane of $\langle a_{M_L'} a_{M_L}\rangle$ to obtain the relation

$$\langle a_{M_L'}a_{M_L}\rangle = (-1)^{M_L-M_L'}\langle a_{-M_L'}a_{-M_L}\rangle , \qquad (2.43)$$

which is used to reduce the number and complexity of terms in the final expression for the coincidence rate.

v.) Next the polarization vector is expressed in terms of spherical-tensor components, ε_q, which are functions of θ', ϕ', and the measured polarization angle β. With the dipole length operator expressed in spherical tensor components X_q^1, as well; the Wigner-Eckert theorem[49] is applied to the resulting matrix elements:

$$\langle L_0M_{L_0}S_0M_{S_0}I_0M_{I_0}|X_{q'}^1|LM_L'SM_SIM_I\rangle^* \times$$

$$\langle L_0M_{L_0}S_0M_{S_0}I_0M_{I_0}|X_q^1|LM_LSM_SIM_I\rangle =$$

$$\frac{|\langle L||X^1||L_0\rangle|^2}{2L+1}\langle L_0M_{L_0}1q'|L_01LM_L'\rangle \times$$

$$\langle L_0M_{L_0}1q|L_01LM_L\rangle . \qquad (2.44)$$

Here, the Clebsch-Gordon coefficients contain the geometrical dependence and the reduced matrix element $\langle L||X^1||L_0\rangle$ depends only on the dynamics of the electromagnetic transition.

vi.) Finally, these results are all used in Eq. (2.30) to obtain an expression for the coincidence rate:

$$\frac{dN}{d\Omega d\Omega'} = vn_0 n_A \left(\frac{3\gamma'}{8\pi}\right)\Big\{A_{00}\cos^2\beta + A_{11}\sin^2\beta + (A_{11}-A_{00})\cos^2\beta\cos^2\theta' + \sqrt{2}\, R_e A_{01}[\sin 2\theta' \times \cos^2\beta\cos(\phi-\phi') + \sin 2\beta\sin\theta'\sin(\phi-\phi')] - R_e A_{1-1}[\cos^2\beta\cos^2\theta' - \sin^2\beta)\cos 2(\phi-\phi') + \sin 2\beta\cos\theta'\sin 2(\phi-\phi')]\Big\} \qquad (2.45)$$

where

$$A_{qq'} = \sum_{JFJ'F'M_L M_L'} U(qq'M_L M_L' JFJ'F'LL_0)\langle a_{M_L'} a_{M_L}\rangle \times \int_0^{\Delta t} dt e^{-(\gamma+i\omega_{JFJ'F'})t} \qquad (2.46)$$

and

$$U(qq'M_L M_L' JFJ'F'LL_0) = \sum_{M_F M_F' M_J M_J' \bar{M}_J' \bar{M}_J M_S M_I} \{\langle L\bar{M}_L SM_{S_0}|LSJM_J\rangle\langle JM_J IM_{I_0}|JIFM_I\rangle \times M_{L_0} M_{I_0} M_{S_0} \bar{M}_L \bar{M}_L'\}$$

$$\langle L_0 M_{L_0} 1q|L_0 1 L\bar{M}_L\rangle\langle L\bar{M}_L, SM_{S_0}|LSJ'M_J,\rangle\langle J'M_J, IM_{I_0}|J'IF'M_F'\rangle \times$$

$$\langle L_0 M_{L_0} 1q'|L_0 1 L\bar{M}_L,\rangle\langle LM_L SM_S|LSJ\bar{M}_J\rangle\langle J\bar{M}_J IM_I|JIFM_F\rangle \times$$

$$\langle LM_L' SM_S|LSJ'\bar{M}_J'\rangle\langle J'\bar{M}_J' IM_I|J'IF'M_F'\rangle[(2S+1)(2I+1)]^{-1} \qquad (2.47)$$

and

$$\gamma' = \frac{8\pi}{3}\frac{e^2\omega^2}{hc^3}\frac{|\langle L||X^1||L_0\rangle|^2}{(2L+1)}\ , \qquad (2.48)$$

where the quantity γ' is equal to the decay width γ times the branching ratio for the decay.

Equation (2.47) can be simplified considerably. MJ gives the simplified form as

$$U(qq'M_L M_L' JFJ'F'LL_0) = (2J+1)(2J'+1)(2F+1)(2F'+1)(2L+1)\times$$
$$[(2S+1)(2I+1)]^{-1}\ (-1)^{L_0+q-M_L}\times$$
$$\sum_{X\nu}(2X+1)(-1)^{-X}\begin{Bmatrix} L & L & X \\ J' & J & S\end{Bmatrix}^2\begin{Bmatrix} J & J' & X \\ F' & F & I\end{Bmatrix}^2\begin{Bmatrix} L & L & X \\ 1 & 1 & L_0\end{Bmatrix}\begin{pmatrix} L & L & X \\ -M_L' & M_L & \nu\end{pmatrix}\begin{pmatrix} 1 & 1 & X \\ -q & q' & -\nu\end{pmatrix}. \qquad (2.49)$$

The coincidence expression (Eq. (2.45)) can be understood by considering the defining equation for $A_{qq'}$, Eq. (2.46). This equation consists of three distinct kinds of terms: the U coefficients, the excitation amplitudes, and the time integral. The effect of the integral is rather clear, i.e., it relates the number of expected decays to the "time window" for detecting a coincidence of the apparatus as well as expressing the interference effects of the decaying coherent states. The excitation amplitudes, $\langle a_{M_L'} a_{M_L}\rangle$, are equivalent to the density matrix elements for the excitation. The U coefficients depend on the intermediate and final states of the atom, as well as on the polarization of the emitted photon (via the q,q' dependence). Thus the quantities

$A_{qq'}$ depend on both the excitation and decay of the states, and may be used to express all the information that can be obtained from a coincidence measurement. These quantities are discussed further in Chapter III.

For the analysis of an experiment in which no polarization measurement is made, Eq. (2.45) is summed over the two perpendicular polarization angles β and $\beta + \frac{\pi}{2}$ to obtain

$$\frac{dN}{d\Omega d\Omega'} = vn_0 n_A \gamma' \frac{3}{8\pi}[A_{00}+A_{11}+(A_{11}-A_{00})\cos^2\theta' + \sqrt{2}\, R_e A_{01}\sin 2\theta'\cos(\phi-\phi') + A_{1-1}\sin^2\theta'\cos 2(\phi-\phi')] . \tag{2.50}$$

4. LS Coupling Violated

MJ also presents formulas for $A_{qq'}$ and U when the radiating atom does not obey LS coupling. In this case, the scattering amplitudes are referred to the J,M_J levels so that

$$A_{qq'} = \sum_{FF'M_JM_J'} U(qq'M_JM_J'FF'JJ_0)\langle a_{M_J'} a_{M_J}\rangle \times \int_0^{\Delta t} dt \exp[-(\gamma+i\omega_{F,F'})t] \tag{2.51}$$

with U defined by

$$U(qq'M_JM_J'FF'JJ_0) = [(2F+1)(2F'+1)(2J+1)/(2I+1)] \times (-1)^{J_0+q-M_J} \sum_{\chi\nu} (2\chi+1)(-1)^{-\chi} \begin{Bmatrix} J & J & \chi \\ F' & F & I \end{Bmatrix}^2 \begin{Bmatrix} J & J & \chi \\ 1 & 1 & J_0 \end{Bmatrix} \begin{pmatrix} J & J & \chi \\ -M_J' & M_J & \nu \end{pmatrix} \begin{pmatrix} 1 & 1 & \chi \\ -q & q' & -\nu \end{pmatrix}. \tag{2.52}$$

In this last equation we have corrected a typographical error in the original paper. Also, the angular momentum L_0, found

in MJ Eq. (17), should be identified with ℓ_6 rather than k_6 in their general expression for U.

In following the method given in the appendix of MJ for the reduction of Eq. (2.47) to the form in Eq. (2.49), we disagree with some of the phases given in intermediate steps. We note that these differences do not affect the final answer. We have found a simpler way to accomplish the reduction from Eq. (2.47) to (2.49) which avoids the use of the 18-j coefficient. This reduction is given in detail in Appendix III with the proper associations for the atomic case.

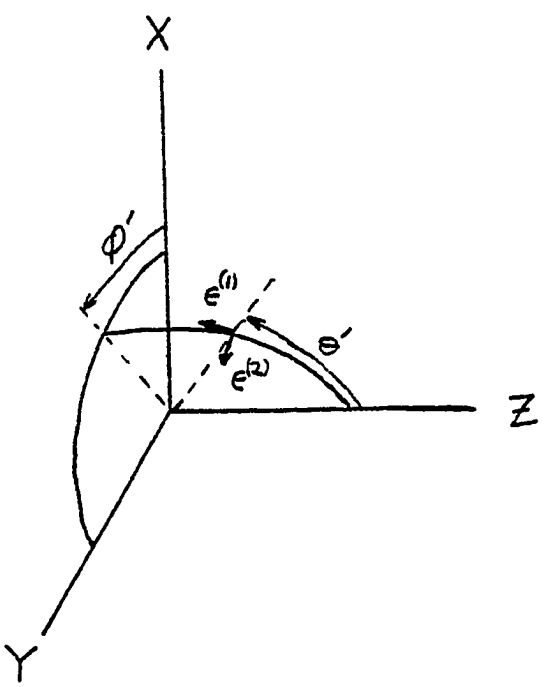

Fig. 2. Polarization unit vectors.

CHAPTER III

ELECTRON-PHOTON COINCIDENCES IN MOLECULAR SCATTERING

In the scattering process

$$e + M \rightarrow M^{**} + e' \tag{2.1}$$

and

$$M^{**} \rightarrow M^{*} + h\nu \ , \tag{2.2}$$

much information may be obtained from a measurement of the angular correlation between the scattered electron, e', and the photon, $h\nu$, and/or the measurement of photon polarization. The purpose of this chapter is to construct a theory for such measurements when the target M (see Eq. (2.1)) is a diatomic molecule: that is, expressing the coincidence rate in terms of detector positions, photon polarizations, and excitation amplitudes for intermediate states.

The quantitative results obtained later in this chapter involves the excitation amplitudes for the various magnetic sublevels of the rotational states. In general, the amplitudes for exciting different sublevels will not be equal, so there will be an unequal population of the magnetic sublevels

for the molecular ensemble.*

Radiation emitted from such an ensemble of molecules is polarized as well as having an anisotropic angular distribution. This is demonstrated by the following simple example: Suppose a molecule in a $^1\Sigma$ state with rotations angular momentum K=1, with M_K=1 emits a photon in the positive z direction as shown in Fig. 3.

In Fig. 3a the diatomic molecule has one unit of angular momentum (+1h) directed along the positive z axis. A dipole transition must have $|11\rangle \rightarrow |00\rangle$. Since the final state has K=0 and M_K=0, the photon must be right-circularly polarized, (RCP), in order to conserve the z-component of angular momentum. If emitted in the -z direction, it would have to be left-circularly polarized, (LCP). If the initial value of M_K=-1, the above polarization would be reversed. The angular distribution of radiation intensity will be that characteristic of the electric dipole radiation.

A. Initial Assumptions

We begin with the statement of a set of initial assumptions. These assumptions are reexamined after the theory is developed.

---

*If the populations are the same for M_K and $-M_K$, but are unequal to that of M_0, the molecules are said to be "aligned". If all the sublevels are unequally populated, the molecules are said to be "oriented".

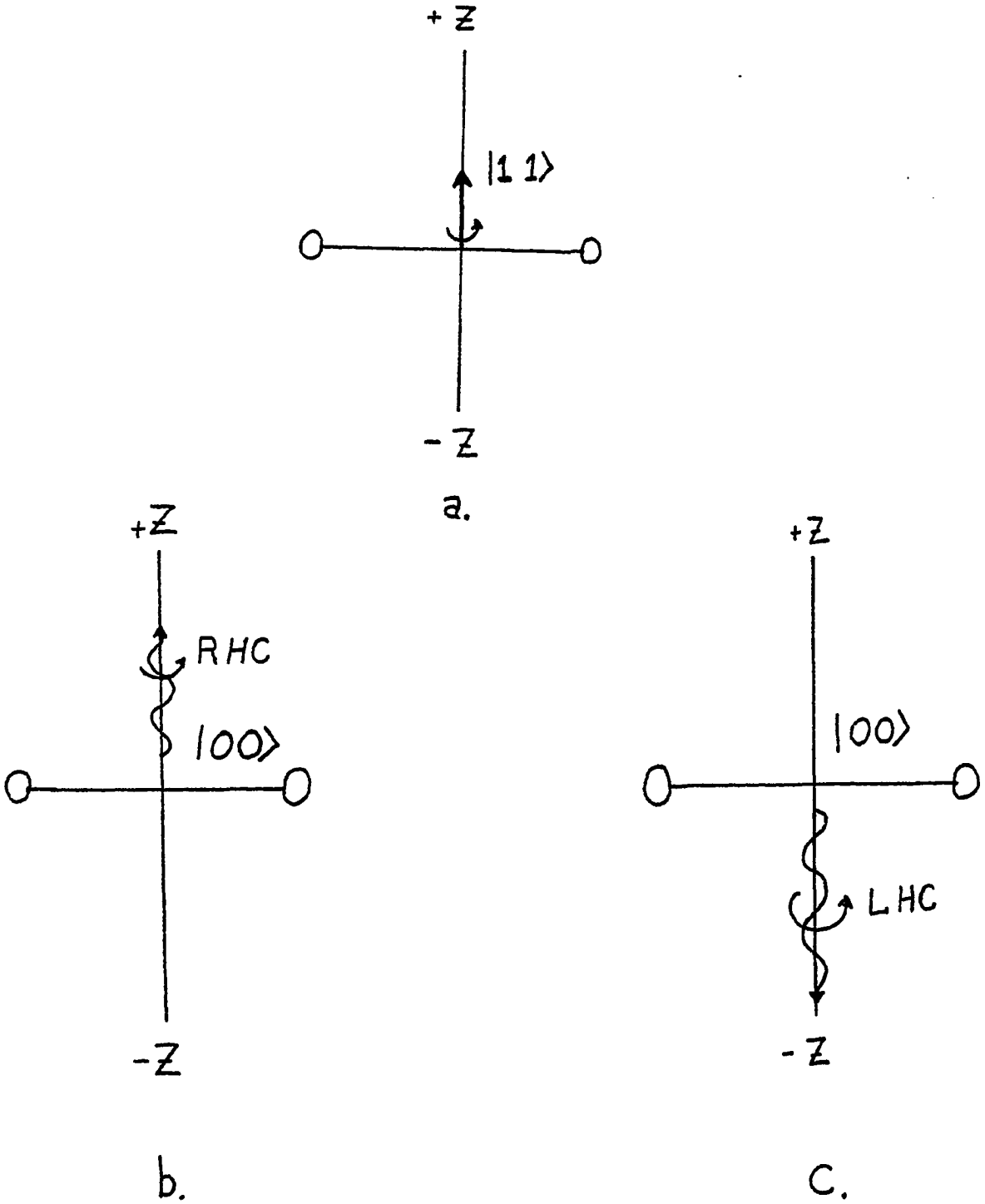

Fig. 3. (a.) Molecule in initial state K=1, M_K=+1. (b.) Dipole radiation allows emission of RHC photon along +Z axis, or (c.) emission of LHC photon along -Z axis.

1. The duration of the collision is short compared to the mean lifetime of the excited molecular state.

This is analogous to the assumption made in the case of electron-atom scattering. If there is no resonant behavior, the duration of the collision has the same order of magnitude as the time required for the electron to travel a distance comparable to a few molecular diameters. The lifetimes of the excited states of interest for this type of experiment are on the order of a few nanoseconds, while the duration of the collision is on the order of 10^{-15} - 10^{-16} seconds. Therefore the scattered electron should have no appreciable effect on the photon emission, so that we may treat the excitation and decay processes separately.

2. Hund's case (b) coupling[50] is adequate to describe the angular momentum coupling of the molecule.

This angular momentum coupling scheme is illustrated in Fig. 4, using the vector model. Here, the electronic orbital angular momentum is strongly coupled to the internuclear exis with projection $|M_L| \equiv \Lambda$. The molecular rotational angular momentum, N, which is orthogonal to the internuclear axis, is coupled to Λ to form the resultant $\vec{K}$. States defined by the quantum number K are referred to as rotational states in the remainder of this work. $\vec{K}$ is coupled to the total electron spin $\vec{S}$, to form the total <u>electronic plus rotational</u> angular momentum $\vec{J}$. The total nuclear spin, $\vec{I}$, is then coupled to $\vec{J}$ to form the total <u>molecular</u> angular momen-

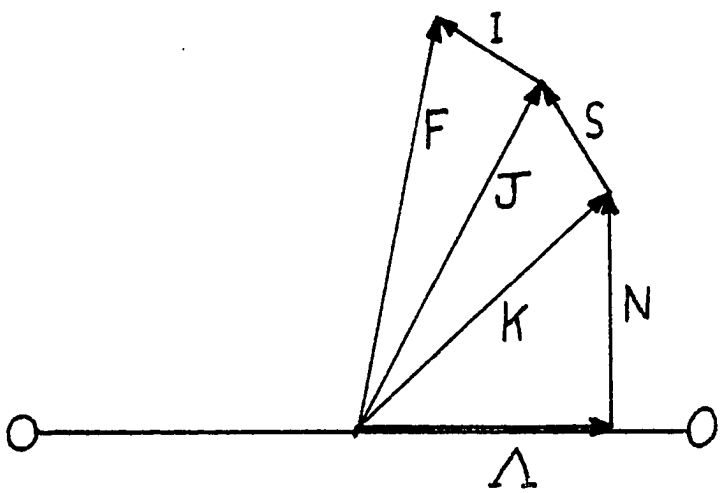

Fig. 4. Schematic diagram of Hund's Case (b) Coupling.

tum $\vec{F}$. The main reason for choosing case (b) coupling is that most of the lighter diatomic molecules obey this coupling scheme; these are the molecules for which rotational levels may be resolved in a measurement.

3. The photon detector has sufficient resolution to distinguish between different values of K, but cannot resolve different values of the magnetic substate, M_K.

4. Hyperfine interactions may be neglected.

This is obviously valid if $\vec{I}=0$, and is reasonable if the hyperfine splitting is small. This assumption permits us to treat $\vec{J}$ as a conserved quantity.

5. The observation time of the measurement is long enough so that "quantum beats" are averaged out over many cycles.

6. The scattering Hamiltonian contains no explicit spin-dependent terms, and the spin-orbit interaction of the excited molecular state is negligible.

This is similar to assumption made for the atomic case. It permits the elimination of spin-dependence from excitation amplitudes.

These assumptions are consistent with an analysis of the scattering process that is physically meaningful and both theoretically and experimentally tractable. The effects of relaxing all of these assumptions except 1 and 6 are discussed later.

B. The General Coincidence Rate Expression

The excited state of the molecule immediately after the excitation (time t=0) may be written

$$|\Psi(t=0)\rangle = \sum_{JM_J} f(KJM_J)\,|KJM_J\rangle \tag{3.1}$$

where $f(KJM_J)$ is the complex excitation amplitude for exciting the state $|KJM_J\rangle$. We suppress other quantum numbers which do not explicitly enter the analysis; these include inversion symmetry (g or u), reflection symmetry (+ or -), vibrational quantum number (v), and any others needed to define the states. From assumption 3, K is known; for $S\neq 0$, we have a coherent superposition of states with different values of J and M_J. Since the wavefunction is not a stationary state of the system, the state decays exponentially:

$$|\Psi(t)\rangle = \sum_{JM_J} f(KJM_J)\,|KJM_J\rangle\, e^{-\frac{\gamma}{2}t} \tag{3.2}$$

where $\frac{1}{\gamma}$ is the mean lifetime of the excited state and the time t is measured from the instant of excitation. There is no oscillatory term in the exponential because assumption 5 makes its effect negligible in this case.

We limit our consideration to allowed electric dipole transitions because the intensity of higher multipole transitions is too low to be observed in this experiment. The probability of the molecule undergoing a transition from the excited state $|\Psi\rangle$ to the final state $|\mathfrak{F}\rangle$ is proportional to

the square of the matrix element for the dipole transition

$$P_{\Psi\to\mathfrak{F}} = |\langle\mathfrak{F}|\hat{\varepsilon}\cdot\vec{X}|\Psi\rangle|^2 \tag{3.3}$$

where $\vec{\varepsilon}$ is the polarization vector for the photon and $\vec{X}$ is the dipole length (or displacement) operator. We must integrate this transition probability from the time of excitation until the detectors shut off (the resolution time of the apparatus). The number of coincidences, dN, occuring in this interval is given by

$$dN = A[\sum_{\mathfrak{F}} \int_0^{t_1} |\langle\mathfrak{F}|\hat{\varepsilon}\cdot\vec{X}|\Psi\rangle|^2 dt]d\Omega d\Omega' \tag{3.4}$$

where

$$A = \frac{vn_0 ne^2\omega^3}{2\pi hc^3}\ , \tag{3.5}$$

t_1 is the resolution time of the apparatus, v is the incident electron velocity, n_0 is the density of electrons in the beam, n is the density of target molecules, e is the electronic charge, ω is the frequency of the decay photon, h is Planck's constant, and c is the velocity of light. The sum over $\mathfrak{F}$ includes all possible unresolved final states of the molecule. The sum is to be taken <u>after</u> squaring the matrix element. The solid angles for the electron and photon detectors are denoted by $d\Omega$ and $d\Omega'$, respectively.

1. The Uncoupled Representation and Spherical Tensor Components.

The first step is to write the eigenfunctions in the

uncoupled representation. The excited-state eigenfunctions in the uncoupled representation are written

$$|KJM_J\rangle = \sum_{\bar{M}_K\bar{M}_S} |K\bar{M}_K S\bar{M}_S\rangle\langle K\bar{M}_K S\bar{M}_S|KSJM_J\rangle \ . \tag{3.6}$$

We also define excitation amplitudes in the new basis by

$$f(KJM_J) = \sum_{M_K M_S} f(KM_K SM_S)\langle KM_K SM_S|KSJM_J\rangle \ . \tag{3.7}$$

Substituting Eqs. (3.6) and (3.7) into Eq. (3.2), we have

$$|\Psi\rangle = \sum_{\bar{M}_K\bar{M}_S M_K M_S} \langle K\bar{M}_K S\bar{M}_S|KSJM_J\rangle\langle KM_K SM_S|KSJM_J\rangle \times f(KM_K SM_S)|K\bar{M}_K S\bar{M}_S\rangle e^{-\frac{\gamma}{2}t} \tag{3.8}$$

in terms of the uncoupled representation.

Now we write the polarization vector $\hat{\varepsilon}$ in the spherical basis, with complex unit vectors

$$\hat{e}_{\pm 1} = \pm\frac{1}{\sqrt{2}}(\hat{e}_x \pm i\hat{e}_y) \tag{3.9a}$$

$$\hat{e}_0 = \hat{e}_z \ , \tag{3.9b}$$

which satisfy

$$\hat{e}_q^* = (-1)^q \hat{e}_{-q} \ , \tag{3.10a}$$

and

$$\hat{e}_q^* \cdot \hat{e}_{q'} = (-1)^q \hat{e}_q \cdot \hat{e}_{-q'} = \delta_{qq'} \ . \tag{3.10b}$$

In this basis a vector $\vec{V}$ is expanded in components as

$$\vec{V} = \sum_q (-1)^q V_q \hat{e}_{-q} \ , \tag{3.11a}$$

where

$$V_q = \hat{e}_q \cdot \vec{V} \ . \tag{3.11b}$$

Next we substitute the uncoupled representation of $|\Psi>$ given by Eq. (3.8), and the spherical tensor expansions of $\vec{\varepsilon}$ and $\vec{X}$ defined by Eq. (3.11) into Eq. (3.4). After squaring the matrix element, and explicitly writing the sum over $\mathcal{F}$ we obtain

$$\frac{dN}{d\Omega d\Omega'} = A \sum_{\substack{\{M_K M'_K M_S M_J M'_J J J' \bar{M}_S \\ M_{S_{\mathcal{F}}} M_{J_{\mathcal{F}}} q q' M_{K_{\mathcal{F}}} \bar{M}_K \bar{M}'_K\}}} (-1)^{q+q'} \varepsilon^*_{-q'} \varepsilon_{-q} <K_{\mathcal{F}} M_{K_{\mathcal{F}}} S_{\mathcal{F}} M_{S_{\mathcal{F}}} | X^1_q | , | K\bar{M}'_K S\bar{M}_S>^* \times$$

$$\times <K_{\mathcal{F}} M_{K_{\mathcal{F}}} S M_{S_{\mathcal{F}}} | X^1_q | K\bar{M}_K S\bar{M}_S> f^*(KM'_K SM'_S) f(KM_K SM_S)$$

$$\times <K\bar{M}'_K S\bar{M}_S | KSJ'\bar{M}'_J><K\bar{M}_K S\bar{M}_S | KSJ\bar{M}_J> \times$$

$$\times <KM'_K SM_S | KSJ'M'_J><KM_K SM_S | KSJM_J> \int_0^{t_1} e^{-\gamma t} \, dt \tag{3.12}$$

where A is defined as in Eq. (3.5)

$$A = \frac{v n_0 n_A e^2 \omega^2}{2\pi h c^3} \ . \tag{3.5}$$

Primed and unprimed excited-state quantum numbers appear since we have a coherent mixture of a number of states. For example, K is known and S is known, but the orientations of these angular momenta are not known. Since

$$J = K+S, \ K+S-1, \ \ldots, \ |K-S| \tag{3.13}$$

and

$$M_J = M_K + M_S, \quad M_K = K, K-1, \ldots, -K, \tag{3.14}$$

$$M_S = S, S-1, \ldots, -S \ , \tag{3.15}$$

it is necessary to sum over these different possible angular momenta, thus giving rise to the different possible J states. Likewise, q and q' imply that different polarizations of the decay photon are possible from the excited states.

2. Applying the Wigner-Eckert Theorem.

Next, we apply the Wigner-Eckart Theorem to the matrix elements of Eq. (3.12), as well as using the Hermitian properties of these matrix elements, to obtain

$$\langle K_{\mathcal{J}} M_K S_{\mathcal{J}} M_{S_{\mathcal{J}}} | X_{q'} | K \bar{M}'_K S M_S \rangle^* \times$$

$$\langle K_{\mathcal{J}} M_K S_{\mathcal{J}} M_{S_{\mathcal{J}}} | X_q | K M_K S M_S \rangle$$

$$= \frac{|\langle K || X^1 || K_{\mathcal{J}} \rangle|^2}{2K+1} \langle K_{\mathcal{J}} M_K 1 q' | K_{\mathcal{J}} 1 K \bar{M}'_K \rangle \times$$

$$\times \langle K_{\mathcal{J}} M_K 1 q | K_{\mathcal{J}} 1 K \bar{M}_K \rangle . \qquad (3.16)$$

The double-barred matrix element, called the reduced matrix element, is characteristic of the transition $K \to K_{\mathcal{J}}$, and does not depend on components q, or projections M_K. The spin-dependence of the matrix elements is suppressed because electric dipole transitions are independent of the spin. The dependence on the geometry of the scattering event is contained in the two Clebsch-Gordan coefficients.

3. ϕ Dependence of the Excitation Amplitudes.

The excitation amplitudes depend on the coordinates θ and ϕ. In this section the ϕ dependence is factored out.

The excitation amplitudes appear as a product, f*f, which is proportional to a product of T matrix elements:

$$f^*(KM_K'SM_S')f(KM_KSM_S) \propto$$

$$\langle \vec{p}_i 0|T|\vec{p}_f KM_K'SM_S'\rangle^* \langle \vec{p}_i 0|T|\vec{p}_f KM_KSM_S\rangle \ . \qquad (3.17)$$

Here, 0 denotes the initial molecular state, which is the same state in <u>both</u> matrix elements. Since we assume (assumption 6) that the spin is unaffected by the collision, and that spin-orbit effects are negligible, we require that

$$M_S = M_S' \ . \qquad (3.18)$$

Now consider the effect of rotating the product of matrix elements in Eq. (3.17) about the z axis: A rotation about $\hat{z}$ by an angle ϕ applied to an eigenket or eigenbra of angular momentum results in

$$\hat{R}_{\hat{z}}(\phi)|jm\rangle = e^{im\phi}|jm\rangle \ , \qquad (3.19)$$

and

$$\langle jm|\hat{R}_z(\phi) = e^{-im\phi}\langle jm| \ , \qquad (3.20)$$

respectively. Thus, when the matrix elements of Eq. (3.17) are rotated together, the effects on bras and kets of 0 and S cancel. The scattered electron momentum, $\vec{p}_f$, always appears in a dot product with $\vec{r}$, the spatial coordinate variable, and is therefore unaffected by the rotation. The net effect of the rotation is

$$\hat{R}_{\hat{z}}(\phi)f^*(KM_K'SM_S')f(KM_KSM_S) =$$

$$e^{i\phi(M_K - M_K')} f^*(KM_K'SM_S')f(KM_KSM_S) \quad . \tag{3.21}$$

This product of amplitudes must be averaged over undetermined initial-state quantum numbers. With the assumptions made, this means averaging over M_S and M_K. Denoting this average by $\int$, we write

$$\int f^*(KM_K'SM_S')f(KM_KSM_S) =$$

$$\delta_{M_SM_S'}(2S+1)^{-1} e^{i\phi(M_K - M_K')} \langle f_{M_K'} f_{M_K} \rangle \quad , \tag{3.22}$$

where the average is now over the quantities enclosed in brackets. The quantity f_{M_K} differs from $f(KM_KSM_S)$ in two important ways: (i.) f_{M_K} is a function of θ only, and, (ii.) f_{M_K} is normalized so that $|f_{M_K}|^2 = \frac{d\sigma_{M_K}}{d\Omega}$. For the remainder of this work, we denote this partial differential cross section for exciting the M_K^{th} magnetic sublevel as σ_{M_K}.

4. Reflection symmetry of $\langle f_{M_K'} f_{M_K} \rangle$.

The reflection properties of $\langle f_{M_K'} f_{M_K} \rangle$ are useful in simplifying some expressions derived later in this chapter.

We choose the x-z plane to be the scattering plane defined by $\vec{p}_i$ and $\vec{p}_f$, so that the coordinate ϕ measures the angle out of the scattering plane. Since $\langle f_{M_K'} f_{M_K} \rangle$ does not depend on ϕ, this excitation amplitude must be invariant to a reflection through the xz plane.

Letting $\hat{M}_{xz}$ be this reflection operator, we express this invariance by

$$\hat{M}_{xz}\langle f_{M_K'} f_{M_K}\rangle = \langle f_{M_K'} f_{M_K}\rangle \ . \tag{3.23}$$

The transformation properties of the excitation amplitudes are the same as those of the T matrix elements; therefore we consider the transformation

$$|KM_K\rangle \rightarrow \hat{M}_{xz}|KM_K\rangle \ . \tag{3.24}$$

The reflection operator $\hat{M}_{xz}$ is equivalent to an inversion followed by a rotation of π radians about the $\hat{y}$ axis:

$$\hat{M}_{xz} = \hat{R}_{\hat{y}}(\pi)\hat{\imath} \ . \tag{3.25}$$

The kets $|KM_K\rangle$ are proportional to spherical harmonics; since we have[47]

$$\hat{\imath}Y_{\ell m} = (-1)^{\ell}Y_{\ell m} \ , \tag{3.26}$$

then

$$\hat{\imath}|KM_K\rangle = (-1)^K|KM_K\rangle \ . \tag{3.27}$$

The rotation by π about the $\hat{y}$ axis may be written as[45]

$$\hat{R}_{\hat{y}}(\pi)|KM_K\rangle = \sum_{m'}|Km'\rangle d^K_{M_K m'}(\pi) \tag{3.28}$$

and with the symmetry

$$d^J_{mk}(\pi) = (-1)^{J-k}\delta_{k,-m} \tag{3.29}$$

gives us

$$\hat{R}_{\hat{y}}(\pi)|KM_K\rangle = (-1)^{K+M_K}|K-M_K\rangle \tag{3.30}$$

and

$$\langle KM_K|\hat{R}_{\hat{y}}(\pi) = (-1)^{K-M_K}\langle K-M_K| \ . \tag{3.31}$$

Combining these results, we obtain

$$\hat{M}_{xz}\langle f_{M'_K} f_{M_K}\rangle = (-1)^{4K}(-1)^{M_K - M'_K}\langle f_{-M'_K} f_{-M_K}\rangle \tag{3.32}$$

Since 4K is an even integer, we can write

$$\langle f_{M'_K} f_{M_K}\rangle = (-1)^{M_K - M'_K}\langle f_{-M'_K} f_{-M_K}\rangle \, . \tag{3.33}$$

5. Polarization.

We write the polarization vector $\hat{\varepsilon}$, as

$$\hat{\varepsilon} = \hat{\varepsilon}^{(1)}\cos\beta + \hat{\varepsilon}^{(2)}\sin\beta \tag{3.34}$$

where $\hat{\varepsilon}^{(1)}$ and $\hat{\varepsilon}^{(2)}$ are orthogonal unit polarization vectors as shown in Fig. (2). In this basis, $\hat{\varepsilon}^{(1)}$ and $\hat{\varepsilon}^{(2)}$ lie in the directions of increasing θ' and ϕ', respectively. The polarization angle, β, is measured with respect to $\hat{\varepsilon}^{(1)}$.

An examination of Fig. (2) shows us that

$$\hat{\varepsilon}^{(1)} = \cos\theta'\cos\phi'\hat{x} + \cos\theta'\sin\phi'\hat{y} - \sin\theta'\hat{z} \tag{3.35}$$

and

$$\hat{\varepsilon}^{(2)} = -\sin\phi'\hat{x} + \cos\phi'\hat{y} \, . \tag{3.36}$$

Using Eqs. (3.9) and (3.11) we can express $\hat{\varepsilon}^{(1)}$ and $\hat{\varepsilon}^{(2)}$ in spherical components:

$$\varepsilon_1^{(1)} = \frac{-\cos\theta' e^{i\phi'}}{\sqrt{2}} \; ; \quad \varepsilon_0^{(1)} = -\sin\theta' \; ; \quad \varepsilon_{-1}^{(1)} = \frac{\cos\theta' e^{-i\phi'}}{\sqrt{2}} \tag{3.37}$$

$$\varepsilon_1^{(2)} = \frac{-ie^{i\phi'}}{\sqrt{2}} \; ; \quad e_0^{(2)} = 0 \; ; \quad e_{-1}^{(2)} = \frac{-ie^{-i\phi'}}{\sqrt{2}} \, . \tag{3.38}$$

C. Simplification of the Coincidence Formula

The objective in this section is to simplify Eq. (3.12), both to clarify physical content of the equation and to make

the equation computationally manageable.

1. The U Coefficients.

We begin by defining the quantity

$$U(q,q',M_K,M_K',J,J') \equiv$$

$$(2S+1)^{-1} \sum_{M_S M_J M_J' \bar{M}_S M_{K_f} \bar{M}_K \bar{M}_K'} <K\bar{M}_K' S\bar{M}_S | KSJ'M_J'><K\bar{M}_K S\bar{M}_S | KSJM_J> \times$$

$$<KM_K' SM_S | KSJ'M_J'><KM_K SM_S | KSJM_J> \times$$

$$<K_f M_{K_f} 1q' | K_f 1 K\bar{M}_K'><K_f M_{K_f} 1q | K_f 1 K\bar{M}_K> \; . \qquad (3.39)$$

This quantity is the product of the Clebsch-Gordan coefficients appearing in Eqs. (3.12) and (3.14). The sum includes all magnetic quantum numbers not appearing in the excitation amplitudes. We performed this sum using the graphical technique;[44] the details are presented in Appendix II. The result of this reduction is that

$$U(qq'M_K M_K' JJ' KK_f) = \frac{(2J'+1)(2J+1)(2K+1)}{(2S+1)} \times$$

$$(-1)^{K_f+M_K+q} \sum_{\chi\nu} (2\chi+1)(-1)^{\chi} \begin{Bmatrix} 1 & 1 & \chi \\ K & K & K_f \end{Bmatrix} \begin{Bmatrix} K & K & \chi \\ J & J' & S \end{Bmatrix}^2 \times$$

$$\times \begin{pmatrix} 1 & 1 & \chi \\ -q & q' & \nu \end{pmatrix} \begin{pmatrix} K & K & \chi \\ -M_K' & M_K & -\nu \end{pmatrix} \; , \qquad (3.40)$$

where the brackets denote Wigner 6j-coefficients and the parentheses denote Wigner 3j-coefficients. The simplification here is considerable, since the sum is only over two indices now rather than over seven. The summation index χ

can have only the values 0,1,2 by the triangle rule of the 3j coefficients, with similar restriction on the possible values of its projection $\nu=0,\pm1,\pm2$, which are determined by the sum rules:

$$-q + q' + \nu = 0 \tag{3.41}$$

$$-M_K' + M_K - \nu = 0 \ . \tag{3.42}$$

Adding these two equations, we get

$$-q + q' = M_K' - M_K \ . \tag{3.43}$$

Clearly this expression is invariant to the change-of-sign of all four quantities; also it is invariant to the simultaneous interchange of q for q' and M_K for M_K'. This establishes the symmetries for U, which are useful in calculations of U for specific transitions. Wigner coefficients may be evaluated by using the computer program listed in Appendix III.

2. The $A_{qq'}$ Coefficients.

Next we define the quantities $A_{qq'}$ in terms of the U's. The $A_{qq'}$ include the dependence on the scattering amplitudes in addition to the time dependence of the radiation. We define

$$A_{qq'} \equiv \sum_{JJ'M_KM_{K'}} U(q,q',M_K,M_{K'},J,J')\langle f_{M_K'} f_{M_K}\rangle(1 - e^{-\gamma t_1}) \tag{3.44}$$

where we have performed the time integration and evaluated it between the limits of $t=0,t_1$.

To determine how many of these $A_{qq'}$ are independent, we consider the symmetry properties of the coefficients U, the reflection symmetry of the excitation amplitudes,

$$\langle f_{M'_K} f_{M_K} \rangle = (-1)^{M_K - M'_K} \langle f_{-M'_K} f_{-M_K} \rangle \ , \tag{3.33}$$

and the Hermitian character of $\langle f_{M'_K} f_{M_K} \rangle$:

$$\langle f_{M'_K} f_{M_K} \rangle = \langle f_{M_K} f_{M'_K} \rangle^* \ , \tag{3.45}$$

for each of the $A_{qq'}$. We find the relations

$$A_{1-1} = A_{-11} \ , \tag{3.46}$$

and

$$A_{1-1} = A_{-11}^* \ , \tag{3.47}$$

or

$$A_{-11} = A_{-11}^* \ , \tag{3.48}$$

which implies that A_{1-1} is real; in addition,

$$A_{11} = A_{-1-1} \text{ (both are real)}, \tag{3.49}$$

$$A_{10} = A_{01}^* \ , \tag{3.50}$$

$$A_{10} = -A_{-10} \ , \tag{3.51}$$

and

$$A_{10} = A_{0-1}^* \ . \tag{3.52}$$

Substitutions among these equations gives

$$A_{-10} = -A_{01}^* \tag{3.53}$$

$$A_{0-1} = -A_{01} \ , \tag{3.54}$$

and that A_{00} is real.

Because of these relations, there are only four independent quantities here; we choose the independent quantities A_{00}, A_{11}, A_{1-1}, and Re A_{01} to describe the scattering.

3. Simplified expression for the coincidence rate.

When we substitute into Eq. (3.12) the results obtained in the preceding sections given by Eqs. (3.16), (3.21), (3.32), (3.37), (3.38), (3.39), and (3.45-3.54), we can write the coincidence rate as

$$dN = B\{A_{00}\cos^2\beta + A_{11}\sin^2\beta + (A_{11}-A_{00}) \times \cos^2\beta\cos^2\theta' + \sqrt{2}\ \mathrm{Re}A_{01}[\sin 2\theta'\cos^2\beta\cos(\phi-\phi') + \sin 2\beta\sin\theta'\sin(\phi-\phi')] - A_{1-1}[(\cos^2\beta\cos^2\theta' - \sin^2\beta)\cos 2(\phi-\phi') + \sin 2\beta\cos\theta'\sin 2(\phi-\phi')]\} . \qquad (3.55)$$

Here, we have defined

$$B = \frac{3\gamma'}{8\pi} v n_0 n_A , \qquad (3.55a)$$

and

$$\gamma' = \frac{8\pi}{3}\frac{e^2\omega^2}{hc^3}\,|\langle K||X^1||K_{\not f}\rangle|^2 \qquad (3.55b)$$

The quantity γ' is equal to the decay width, γ, times the branching ratio for the decay. This equation, with the defining equation for $A_{qq'}$ and U, relates the coincidence rate to the polarization of the emitted radiation, the excitation amplitudes, and the angular distribution of the scattered particles.

If no polarization measurements are made of the emitted radiation, Eq. (3.55) should be summed over two independent (orthogonal) polarization states. Summing over polarizations $\hat{\varepsilon}^{(1)}$ and $\hat{\varepsilon}^{(2)}$ ($\beta=0$ and $\frac{\pi}{2}$), we obtain

$$dN = B[A_{00} + A_{11} + (A_{11} - A_{00})\cos^2\theta' + \sqrt{2}\,\mathrm{Re}A_{01}\sin 2\theta'\cos(\phi-\phi') + A_{1-1}\sin^2\theta' \times \cos 2(\phi-\phi')]d\Omega d\Omega' \,. \tag{3.56}$$

Eqs. (3.55) and (3.56) may be used in a variety of ways. The density matrix elements for the excitation might be calculated in some approximation and used in Eq. (3.56) to predict a coincidence rate as a function of scattered electron angle. Or, the coincidence rate might be measured experimentally, then fitted to Eq. (3.56) [or to Eq. (3.55) if polarization measurements are made] in order to obtain the excitation amplitudes for various magnetic sublevels of the rotational states. The cross sections for excitation of particular rotational states, which are important for many applications today, are readily obtained once the σ_{M_K}'s are known since

$$\sigma_K = \sum_{M_K} \sigma_{M_K} \,. \tag{3.57}$$

It is also possible to obtain the polarization of the emitted radiation without making a calculation (or measurement) of the polarization by calculating the density matrix elements and using Eq. (3.56) to predict the coincidence rate. This

calculated rate and the density matrix elements may then be used in Eq. (3.55) to determine the polarization angle. Similarly the experimentalist could measure the coincidence rate and use Eq. (3.56) to determine the cross sections, then use these values in Eq. (3.55) to determine the polarization.

D. Further Comments on the Coincidence Formula

An important aspect of the use of Eqs. (3.55) or (3.56) for determining the magnetic sublevel differential cross sections for excitation is the number of parameters (or, equivalently, the number of distinct measurements) necessary for their determination. For some specific detector positions the number of parameters is a minimum.

To demonstrate this, we consider some particular values of ϕ, θ', and ϕ'. If $\theta' = 90°$:

$$dN = B[A_{00} + A_{11} + A_{1-1}\cos 2(\phi-\phi')]d\Omega d\Omega' , \tag{3.58}$$

if $\theta' = 90°$, $\phi-\phi' = 90°$ or $270°$:

$$dN = B[A_{00} + A_{11} - A_{1-1}]d\Omega d\Omega' , \tag{3.59}$$

if $\theta'=90°$, $\phi-\phi'=45°$, $135°$, $225°$, or $315°$:

$$dN = B[A_{00} + A_{11}]d\Omega d\Omega' , \tag{3.60}$$

if $\theta'=90°$, $\phi-\phi'=0°$ or $180°$:

$$dN = B[A_{00} + A_{11} + A_{1-1}]d\Omega d\Omega' , \tag{3.61}$$

if $\phi-\phi'=90°$:

$$dN = B[A_{00} + A_{11} + (A_{11}-A_{00})\cos^2\theta' - A_{1-1}\sin^2\theta']d\Omega d\Omega' . \tag{3.62}$$

We note that because of the symmetry properties of the U's, the quantities A_{00} and A_{11} will not contain any terms of the form $\langle f_{M_K'} f_{M_K} \rangle$ where $M_K' \neq M_K$. This means that A_{00} and A_{11} may always be written as

$$\sum_{i=0}^{K} b_i \sigma_i \ . \tag{3.63}$$

Under some conditions, we can write A_{1-1} in this form, but we can never write A_{01} in this form. The reason is that A_{01} always contains terms of the type $\langle f_{M_K'} f_{M_K} \rangle$ where

$$M_K' = M_K \pm 1 \ , \tag{3.64}$$

Therefore if we choose ϕ-ϕ' and θ' so as to eliminate A_{01} and A_{1-1}, the lowest number of parameters necessary to describe the scattering is obtained, although this loses the information on the relative phases of the excitation amplitudes. As an example, the level K has 2K+1 magnetic sublevels. This implies that we need only to determine 2K+1 parameters: $\sigma_K, \sigma_{K-1}, \ldots, \sigma_0, \ldots, \sigma_{-K}$, where

$$\langle f_{M_K} f_{M_K} \rangle = \sigma_{M_K} \ , \tag{3.65}$$

but, noting that

$$\langle f_{M_K'} f_{M_K} \rangle = (-1)^{M_K - M_K'} \langle f_{-m_K'} f_{-M_K} \rangle \tag{3.33}$$

implies $\sigma_{M_K} = \sigma_{-M_K}$, (3.66)

we reduce the necessary parameters to $\sigma_{M_K}, \sigma_{M_{K-1}}, \ldots, \sigma_0$,

or K+1 parameters. Therefore we require K+1 measurements to determine the magnetic sublevel cross sections for the rotational state K.

We point out that there is an upper limit to the number of parameters that can be determined here. Recall that we are describing the process with the four quantities A_{00}, A_{11}, A_{1-1}, and ReA_{01}, and are therefore limited to determining four quantities from the coincidence measurement. However, if a different final state is taken (such as the P and R branches of an electronic transition), additional parameters may then be determined since the $A_{qq'}$ will be different functions of the excitation amplitudes.

The physical significance of the terms $\langle f_{M_K} f_{M_K} \rangle$ is clear: the complex conjugation removes the phase factor so that this quantity is a real number and is equal to the cross section for exciting the $|K,M_K\rangle$ state. The physical significance of $\langle f_{M_K'} f_{M_K} \rangle$ where $M_K' \neq M_K$ is not quite so obvious, however. Consider the mirror symmetry discussed earlier: we found that

$$f_{M_K} = \hat{M}_{xz} f_{M_K} = (-1)^{2K+M_K} f_{-M_K} = (-1)^{M_K} f_{-M_K} \tag{3.67}$$

since K is an integer. Thus we have

$$f_1 = -f_{-1} \ , \quad f_2 = f_{-2} \ , \quad \text{etc.} \tag{3.68}$$

This leads to

$$\langle f_1 f_{-1} \rangle = -\langle f_1 f_1 \rangle = -\sigma_1 \tag{3.69}$$

and

$$\langle f_2 f_{-2} \rangle = \langle f_2 f_2 \rangle = \sigma_2 \ , \tag{3.70}$$

and so forth. Now consider $\langle f_{M_K'} f_{M_K} \rangle$ where $M_K' \neq \pm M_K$. Since the overall phase of the molecular wavefunction $|\psi\rangle$ is arbitrary we can assign a phase of 0° to f_0, i.e., f_0 is real, and measure the phase of the other excitation amplitudes relative to f_0. That is,

$$f_{M_K} = |f_{M_K}| \, e^{i\chi_{OM_K}} \tag{3.71}$$

where χ_{OM_K} is the relative phase between f_0 and f_{M_K}. In this case

$$|f_{M_K}| = +\sqrt{\sigma_{M_K}} \ , \tag{3.72}$$

implies that

$$f_{M_K} = \sqrt{\sigma_{M_K}} \, e^{i\chi_{OM_K}} \ , \tag{3.73}$$

giving the result

$$\langle f_{M_K'} f_{M_K} \rangle = \sqrt{\sigma_{M_K'} \sigma_{M_K}} \, e^{i(\chi_{OM_K} - \chi_{OM_K'})} \ . \tag{3.74}$$

We see from this that the inclusion of A_{01} in the analysis will add additional parameters (the χ_{OM_K}'s) to the fitting procedure; or, if desired, these relative phases may be determined. This would not be possible without the coherent excitation of the substates. Thus we are able to obtain this information about the scattering process that is not possible to obtain even in a high resolution "direct"

measurement without coincidence detection.

CHAPTER IV

APPLICATION TO THE H_2 MOLECULE

One of the complicating features of molecular physics is the formidable number of closely spaced energy levels. Rosen,[52] for example, lists data of forty-five electronic states of the H_2 molecule, each of which, of course, has ten to twenty vibrational levels (spaced on the order of a few tenths of an electron volt apart). Each of these vibrational levels then has many rotational levels (spaced on the order of a few hundredths of an eV apart).

We have chosen the H_2 molecule to illustrate the theory of Chapter III. Since this molecule has the smallest reduced mass of any molecule, the vibrational and rotational level spacings tend to be larger than for other molecules, so the possibility of experimentally selecting definite values of K is better. Necessary parameters are known for many electronic states, and Hund's case (b) coupling is satisfied by most states.

The target H_2 molecules are assumed to be in the $X^1\Sigma_g^+$ electronic ground state and the v=0 vibrational level. The initial K level may be selected by some experimental

technique such as selective excitation by a laser, or an average might be made over the occupied levels, the distribution of which is usually Boltzmann.

Electron impact can excite practically all of the excited electronic states, although some restrictions have been noted.[53,54]

The photon emission, which we assume to be an electric dipole transition, has very definite angular-momentum selection rules: $K_{\mathcal{F}} = K \pm 1$. In general, A_{00}, A_{11}, A_{1-1}, and A_{01} will have different values for these two transitions, so that we may obtain eight independent parameters by varying θ' and $\phi-\phi'$.

Of course, if the resolution of the photon detector is sufficient to distinguish between the rotational transitions, it will also be able to distinguish between vibrational levels of the intermediate and final states. To first order, we would expect no change in the form of the equations for the angular distribution due to different vibrational levels, other than changes in intensity.

A. The $B'\Sigma_u^+$ State (Lyman Band)

We take as our first example excitation of the $B'\Sigma_u^+$ (v=0) state of H_2, which is the lowest-energy excited state, and is relatively isolated from the other electronic states. This state has a mean lifetime of 0.8 nsec[55] for decays back to the ground state. We assume an observation time of about 5-10 ns so that $\gamma t_1 \approx 0$, then $e^{-\gamma t_1} \approx 1$.

Since this is a singlet state, S=0 and J=J'=K; thus $\Delta K=+1$ (R branch) or $\Delta K=-1$ (P branch). For the case K=0, $K_{\mathcal{J}}=1$ we find

$$A_{00} = \frac{1}{3}\,\sigma_0(\tfrac{1}{\gamma}) \ , \tag{4.1a}$$

$$A_{11} = \frac{1}{3}\,\sigma_0(\tfrac{1}{\gamma}) \ , \tag{4.1b}$$

$$A_{01} = 0 \ , \tag{4.1c}$$

and

$$A_{1-1} = 0 \ , \tag{4.1d}$$

so there is only one independent parameter, $\sigma_0(\theta)$. For the convenient setting, $\theta' = 90°$ we obtain the following simple expression for the coincidence rate:

$$dN(\theta) = \frac{2B}{3\gamma}\,\sigma_0(\theta)d\Omega d\Omega' \ . \tag{4.2}$$

The first excited rotational level, K=1, can decay to either $K_{\mathcal{J}}=0$ or $K_{\mathcal{J}}=2$. The transition to $K_{\mathcal{J}}=0$ gives

$$A_{00} = \sigma_0/\gamma \ , \tag{4.3a}$$

$$A_{11} = \sigma_1/\gamma \ , \tag{4.3b}$$

$$A_{01} = \langle f_0 f_1 \rangle/\gamma \ , \tag{4.3c}$$

and

$$A_{1-1} = -\sigma_1/\gamma \ ; \tag{4.3d}$$

while that to $K_{\mathcal{J}}=2$ gives

$$A_{00} = [\tfrac{2}{5}\,\sigma_0 + \tfrac{3}{5}\,\sigma_1]\tfrac{1}{\gamma} \ , \tag{4.4a}$$

$$A_{11} = [\frac{3}{10}\,\sigma_0 + \frac{7}{10}\,\sigma_1]\frac{1}{\gamma}\,, \tag{4.4b}$$

$$A_{01} = [\frac{1}{10}\,\langle f_0 f_1\rangle]\frac{1}{\gamma}\,, \tag{4.4c}$$

and

$$A_{1-1} = [-\frac{1}{10}\,\sigma_1]\frac{1}{\gamma}\,. \tag{4.4d}$$

Thus, one can obtain the three independent quantities $\sigma_0(\theta)$, $\sigma_1(\theta)$, and $\chi_{01}(\theta)$ with only two settings: say $\theta'=90°$ for both transitions, then a setting of ϕ' for which A_{01} is present in the coincidence equation.

The next rotational state, K=2, decays to $K_f=1$ or $K_f=3$. For $K_f=1$ we obtain:

$$A_{00} = [\frac{2}{3}\,\sigma_0 + \sigma_1]\frac{1}{\gamma}\,, \tag{4.5a}$$

$$A_{11} = [\frac{1}{6}\,\sigma_0 + \frac{1}{2}\,\sigma_1 + \sigma_2]\frac{1}{\gamma}\,, \tag{4.5b}$$

$$A_{1-1} = [-\frac{1}{2}\,\sigma_1 + \frac{\sqrt{6}}{3}\,\mathrm{Re}\langle f_0 f_2\rangle]\frac{1}{\gamma}\,, \tag{4.5c}$$

and

$$A_{01} = [\frac{\sqrt{3}}{3}\,\langle f_0 f_1\rangle + \frac{\sqrt{3}}{6}\,\langle f_{-1} f_0\rangle]\frac{1}{\gamma}\,, \tag{4.5d}$$

while the other case, $K_f=3$, yields

$$A_{00} = [\frac{3}{7}\,\sigma_0 + \frac{16}{21}\,\sigma_1 + \frac{10}{21}\,\sigma_2]\frac{1}{\gamma}\,, \tag{4.6a}$$

$$A_{11} = [\frac{2}{7}\,\sigma_0 + \frac{13}{21}\,\sigma_1 + \frac{16}{21}\,\sigma_2]\frac{1}{\gamma}\,, \tag{4.6b}$$

$$A_{1-1} = [-\frac{1}{7}\,\sigma_1 + \frac{2\sqrt{2}}{\sqrt{147}}\,\mathrm{Re}\langle f_0 f_2\rangle]\frac{1}{\gamma}\,, \tag{4.6c}$$

and

$$A_{01} = [-0.24714\langle f_0 f_1\rangle - \frac{1}{3}\langle f_{-1} f_0\rangle$$

$$- \frac{2\sqrt{2}}{\sqrt{441}} \langle f_1 f_2 \rangle + .3367 \langle f_2 f_1 \rangle] \frac{1}{\gamma} . \qquad (4.6d)$$

There are now five independent parameters: σ_0, σ_1, σ_2, x_{01}, and x_{02}.

If the K=3 state is excited, the decay can go either to $K_f=2$ or $K_f=4$. For $K_f=2$ we obtain

$$A_{00} = [\frac{3}{5} \sigma_0 + \frac{16}{15} \sigma_1 + \frac{2}{3} \sigma_2] \frac{1}{\gamma} , \qquad (4.7a)$$

$$A_{11} = [\frac{1}{5} \sigma_0 + \frac{7}{15} \sigma_1 + \frac{2}{3} \sigma_2 + \sigma_3] \frac{1}{\gamma} , \qquad (4.7b)$$

$$A_{1-1} = [-\frac{2}{5} \sigma_1 + \frac{2\sqrt{2}}{\sqrt{15}} \mathrm{Re}\langle f_2 f_0 \rangle + \frac{2}{\sqrt{15}} \mathrm{Re}\langle f_3 f_1 \rangle] \frac{1}{\gamma} , \qquad (4.7c)$$

and

$$A_{01} = [0.4899 \langle f_0 f_1 \rangle + 0.3266 \langle f_{-1} f_0 \rangle + 0.5963 \langle f_1 f_2 \rangle + 0.1491 \langle f_{-2} f_{-1} \rangle + \frac{\sqrt{3}}{3} \langle f_2 f_3 \rangle] \frac{1}{\gamma} . \qquad (4.7d)$$

While for $K_f=4$ we obtain

$$A_{00} = [\frac{4}{9} \sigma_0 + \frac{5}{6} \sigma_1 + \frac{2}{3} \sigma_2 + \frac{7}{18} \sigma_3] \frac{1}{\gamma} , \qquad (4.8a)$$

$$A_{11} = [\frac{5}{18} \sigma_0 + \frac{7}{12} \sigma_1 + \frac{2}{3} \sigma_2 + \frac{29}{36} \sigma_3] \frac{1}{\gamma} , \qquad (4.8b)$$

$$A_{1-1} = [-\frac{1}{6} \sigma_1 + 2 \frac{\sqrt{5}}{\sqrt{216}} \mathrm{Re}\langle f_2 f_0 \rangle + 2\sqrt{\frac{5}{432}} \mathrm{Re}\langle f_3 f_1 \rangle] \frac{1}{\gamma} , \qquad (4.8c)$$

and

$$A_{01} = [+0.3402 \langle f_1 f_0 \rangle - 0.2722 \langle f_0 f_1 \rangle - \frac{5}{12}\sqrt{5} \langle f_1 f_2 \rangle + \frac{5}{6} \sqrt{5} \langle f_2 f_1 \rangle - 0.0962 \langle f_2 f_3 \rangle + 0.3368 \langle f_3 f_2 \rangle] \frac{1}{\gamma} . \qquad (4.8d)$$

The number of independent parameters is now seven: σ_0, σ_1, σ_2, σ_3, χ_{01}, χ_{02}, χ_{03}.

Obviously the quantities $A_{qq'}$ can be calculated with little difficulty for much higher values. However, the number of independent parameters will exceed the number which can be experimentally determined.

B. The $C'\Pi_u$ State (Werner bands)

A more complicated example results from exciting the $C'\Pi_u$ electronic state of H_2. Except for $E,F\,^1\Sigma_g^+$, which lies close to $C'\Pi_u$, this state is relatively isolated, and has even larger vibrational-rotational spacings than $B'\Sigma_u^+$.

Of course, Π states have electronic as well as nuclear rotational angular momentum. The $C'\Pi_u$ state decays to the ground electronic state with a mean lifetime of approximately 0.88 ns. Since this is a $\Pi\rightarrow\Sigma$ transition, the dipole selection rules allow the P, Q, and R branches, thus providing a maximum of twelve parameters to describe the process.

Another feature of Π states should also be mentioned: Λ-doubling. For a state with $\Lambda \neq 0$, there is a slight splitting of the electronic levels into two states denoted by Λ^+ and Λ^-. This splitting, called Λ-type doubling, increases as N increases. (This effect is negligible for the state we are considering, but should be considered when applying this theory to other states, particularly of heavier molecules.)

The values of the U's for the P and R branches are the same as in the preceding example, thus the $A_{qq'}$'s for these branches are the same function of the excitation amplitudes as in the previous example. The $A_{qq'}$'s for the Q branch may be readily calculated in the same way.

C. Experimental Feasibility

Since this work is intended to be useful for analyzing experimental data, it is quite legitimate to ask "Is this proposed measurement possible with presently or prospectively available apparatus?" In this section we consider this question and make some estimates of necessary parameters for the experiment.

We divide this question into two parts. First, can sufficiently high counting rates be expected so that the measurement may be made in a reasonable length of time? Second, can sufficient resolution be obtained to select a particular transition for study?

1. Estimated Counting Rate.

We will use the $B'\Sigma_u^+$ state discussed in section A of this chapter as an example. Some of the magnitudes for the experimental parameters used in what follows are taken from the description of experimental apparatus in the literature, others are estimated with the help of experimentalists working with coincidence experiments.

Because we require that the apparatus resolve rotational levels, the photon intensity will be low. Since the

lifetime of this state is less than a nanosecond, all the molecules excited will decay while the detectors are "on".

For the purpose of making this estimate, we assume that the radiation is spatially isotropic, so that the coincidence rate is given by

$$dN \approx \frac{J_e n_0}{e} V \sigma_K \, d\Omega' d\Omega \qquad (4.9)$$

where J_e is the electron current density, n_0 is the target density, e is the electronic charge, V is the interaction volume, and σ_K is the cross section for exciting the K^{th} rotational level, followed by a decay to the final state K . We chose the following parameters:

pressure in gas beam 10^{-4} Torr,

electron beam current 10^{-6} Amp.,

diameter of electron beam 0.1 mm,

diameter of gas beam 0.1 cm,

solid angle of photon detector 2.7×10^{-2} sr.,

solid angle of electron detector 2.7×10^{-3} sr.

The interaction volume is approximated as a cylinder 0.1 mm in diameter and 0.1 cm in length.

Substituting into Eq. (4.9) we obtain

$$dN \approx 1.6 \times 10^{20} \sigma_K \quad (\sigma_K \text{ in } cm^2) \, . \qquad (4.10)$$

Since values for σ_K have not been published, we estimate this as follows: The total cross section for 25 eV electrons to excite the $B'\Sigma_u^+$ state is $4 \times 10^{-17} cm^2$.[55] We take the

target molecules to be in the v=0 vibrational level. Using the Franck-Condon factors between the optimum vibrational states ofthe X↔B transitions,[57] we estimate the cross section for the optimum <u>vibrational</u> level to be $\sim 8\times10^{-19}cm^2$. It is a reasonable estimate that the cross section for the rotational excitation is an order of magnitude smaller, i.e.,

$$\sigma_K \approx 8\times10^{-20}cm^2 \ . \qquad (4.11)$$

If we take the efficiency of the combined detection apparatus to be 1%, this gives a count rate of approximately 0.1 counts/second. Although this is a low counting rate, it is not so low as to make the measurement unfeasible.

2. Photon resolution.

We have assumed that the photon detector can resolve the photon wavelengths well enough to select a particular transition ($K\rightarrow K_{\not}$). To check the validity of this assumption, we calculated the energy differences[52] between each of the first five rotational states of $B'\Sigma_u^+(v=0)$ and the corresponding allowed final states of $X'\Sigma_g^+(v=0)$. These transitions are UV, with a wavelength of approximately 1130Å. As a typical example, the transition nearest in energy to the transition

$$K = 1 \rightarrow K_{\not} = 0 \ , \qquad (4.12)$$

is

$$K = 2 \rightarrow K_{\not} = 1 \ . \qquad (4.13)$$

The energy difference between these two transitions is about 5 meV; the corresponding wavelength difference is 0.5Å. This resolution (or higher) has been obtained by several workers.[58-60]

CHAPTER V

MODIFICATIONS OF THE INITIAL ASSUMPTIONS

In this chapter we consider the effects of relaxing some of the initial assumptions made in Chapter III.

A. Hyperfine Structure and Quantum Beats

We simultaneously relax the assumption that no hyperfine structure is present, and the assumption that no quantun beats are observed, since the two assumptions are related. When a molecule has a non-zero total nuclear spin, the resulting hyperfine levels may be coherently excited, giving rise to quantum beats with a frequency such that they may be detected. For example, consider the H_2 molecule: it has two protons (spin 1/2), so that the total nuclear spin is I = 1 or I = 0. The latter may be readily treated by the theory of Chapter III, but the former may have hyperfine structure.

To take this possibility into account we use the additional angular momentum quantum numbers F and I defined in Chapter III (see Fig. 3). The coupled representation for the excited state of the molecule for this case is given by

$$|\Psi(t)\rangle = \sum_{JFM_F} f(KJFM_F)|KJFM_F\rangle e^{-(\frac{\gamma}{2} + \frac{iE_{JF}}{\hbar})t} \qquad (5.1)$$

where the excitation is assumed to have occurred at t = 0. This equation may be compared to Eq. (3.2). There are two distinct differences: First, the total angular momentum is now the quantity F, with projection M_F. The nuclear spin is not strongly coupled to J, so that the component of I is conserved. The effect of this weak coupling is to cause a slight shift in the energy levels. These nearly degenerate levels will be coherently excited. Second, we have introduced an imaginary term in the exponential. This term causes an oscillation in the intensity of the photons emitted from the coherently excited states. If the energy levels are so close that the frequency of the oscillations is low, then the oscillations are not "averaged out" during the observation time. In this case the oscillations, called quantum beats, can be observed experimentally and can be used to determine the fine and hyperfine structure of various atoms and molecules.[61-63]

Since the development is similar to that in Chapter III, we will not repeat the arguments here, but summarize the procedure. First we write the excitation amplitude $f(KJFM_F)$ and the eigenket $|KJFM_J\rangle$ in an uncoupled representation to allow the separation of the electronic spin, as in Chapter III, and the nuclear spin from the excitation amplitudes. The uncoupled representation for the eigenket is

$$|KJFM_F\rangle = \sum_{M_K M_S M_I M_J} |KM_K SM_S IM_I\rangle\langle KM_K SM_S|KSJM_J\rangle \times \times \langle JM_J IM_I|JIFM_F\rangle \, , \qquad (5.2)$$

and for the excitation amplitude by

$$f(KJFM_F) = \sum_{M_K M_S M_I M_J} f(KM_K SM_S IM_I) \langle KM_K SM_S | KSJM_J \rangle \times \langle JM_J IM_I | JIFM_F \rangle \ . \qquad (5.3)$$

Substituting Eqs. (5.2) and (5.3) into the general coincidence rate equation and expanding in spherical-tensor components, we obtain

$$\begin{aligned} dN = A \sum_{\alpha} & f^*(KM_K'SM_S'IM_I') \langle KM_K'SM_S' | KSJ'\bar{M}_J' \rangle \times \\ & \langle J'\bar{M}_J' IM_I' | F'M_F' \rangle f(KM_K SM_S IM_I) \langle KM_K SM_S | KSJ\bar{M}_J \rangle \times \\ & \langle J\bar{M}_J IM_I | JIFM_F \rangle (-1)^{q+q'} \varepsilon^*_{-q'} \varepsilon_{-q} \times \\ & \langle K_{\mathscr{f}} M_{K_{\mathscr{f}}} S_{\mathscr{f}} M_{S_{\mathscr{f}}} I_{\mathscr{f}} M_{I_{\mathscr{f}}} | X^1_{q'} | K\bar{M}_K' SM_S' IM_I' \rangle^* \times \\ & \langle K\bar{M}'_K SM_S' | KSJ'M_J' \rangle \langle J'M_J' IM_I' | J'IF'M_F' \rangle \times \\ & \langle K_{\mathscr{f}} M_{K_{\mathscr{f}}} S_{\mathscr{f}} M_{S_{\mathscr{f}}} I_{\mathscr{f}} M_{I_{\mathscr{f}}} | X^1_q | K\bar{M}_K SM_S IM_I \rangle \times \\ & \langle K\bar{M}_K SM_S | KSJM_J \rangle \langle JM_J IM_I | JIFM_F \rangle \times \\ & \int_0^{t_1} \exp[-(\gamma + i\omega_{JF,J'F'})t] dt \ , \end{aligned} \qquad (5.4)$$

where the sum is over the set

$$\begin{aligned} \alpha \equiv \{ & q, q', J, J', F, F', M_F, M_F', M_S, M_I, M_S', M_I', M_{K_{\mathscr{f}}}, \\ & M_{S_{\mathscr{f}}}, M_{I_{\mathscr{f}}}, \bar{M}_J, \bar{M}_J', \bar{M}_K', \bar{M}_K, M_J', M_J \} \ . \end{aligned} \qquad (5.5)$$

The frequency of the oscillations in the hyperfine structure,

$\omega_{JF,J'F'}$, is defined by

$$\omega_{JF,J'F'} = \frac{E_{JF} - E_{J'F'}}{\hbar} \tag{5.6}$$

Because the nuclear spin projection is conserved, we can write

$$M_I = M'_I \ . \tag{5.7}$$

We redefine the quantity U so as to include the effect of nuclear spin as

$$\begin{aligned} U(q,q',M_K,M'_K,J,J',F,F',K,K_{\mathcal{F}}) \\ \equiv \sum_{\substack{M_F M'_F M_{K_{\mathcal{F}}} \bar{M}_{S_{\mathcal{F}}} M_{I_{\mathcal{F}}} \bar{M}_J \bar{M}'_J \\ \bar{M}'_K \bar{M}_K M'_J M_J M_S M_I}} & \langle KM'_K SM_S | KSJ'\bar{M}'_J \rangle \langle J'\bar{M}'_J IM_I | J'IF'M'_F \rangle \times \\ & \langle KM_K SM_S | KSJ\bar{M}_J \rangle \langle J\bar{M}_J IM_I | JIFM_F \rangle \times \\ & \langle K\bar{M}'_K SM_{S_{\mathcal{F}}} | KSJ'M'_J \rangle \langle J'M'_J IM_{I_{\mathcal{F}}} | J'IF'M'_F \rangle \times \\ & \langle K\bar{M}_K SM_{S_{\mathcal{F}}} | KSJM_J \rangle \langle JM_J IM_{I_{\mathcal{F}}} | JIFM_F \rangle \times \\ & \langle K_{\mathcal{F}} M_{K_{\mathcal{F}}} 1q' | K_{\mathcal{F}} 1 K\bar{M}'_K \rangle \langle K_{\mathcal{F}} M_{K_{\mathcal{F}}} 1q | K_{\mathcal{F}} 1 K\bar{M}_K \rangle \end{aligned} \tag{5.8}$$

This expression may be reduced as in the case without hyperfine structure by the diagrammatic technique. The details are given in Appendix II. We can then write U as

$$U(q,q',M_K,M'_K,J,J',F,F',K,K_{\mathcal{F}}) =$$

$$[(2J+1)(2J'+1)(2F+1)(2F'+1)(2K+1)][(2S+1)(2I+1)]^{-1}$$

$$(-1)^{K_{\mathcal{F}}+q-M_K} \sum_{\chi\nu} (2\chi+1)(-1)^{\chi} \begin{Bmatrix} K & K & \chi \\ J' & J & S \end{Bmatrix}^2 \begin{Bmatrix} J & J' & \chi \\ F' & F & I \end{Bmatrix}^2 \begin{Bmatrix} K & K & \chi \\ 1 & 1 & K_{\mathcal{F}} \end{Bmatrix}$$

$$\begin{pmatrix} K & K & \chi \\ -M_K' & M_K & \nu \end{pmatrix} \begin{pmatrix} 1 & 1 & \chi \\ -q & q' & -\nu \end{pmatrix} , \qquad (5.9)$$

with $A_{qq'}$ also redefined to be

$$A_{qq'} = \sum_{JJ'FF'M_KM_K'} U(qq'M_KM_K'JJ'FF'KK_{\mathcal{F}}) \langle f(KM_K') f(KM_K) \rangle$$

$$\times \int_0^{t_1} \exp[-(\gamma+i\omega_{JF,J'F'})t]dt . \qquad (5.10)$$

We illustrate this theory with an application to the $d^3\Pi_u$ (1s,3p) (Fulcher band) state of H_2. We chose this state because a considerable amount of work has been done on it, including the hyperfine structure of the ortho states. For this state, the hyperfine splitting is larger than the natural linewidth, so the possibility of detecting quantum oscillations is present. The lifetime of this state is given by Cahill[64] as 68±5 ns (for v=0), and by Freund and Miller[65] as 29.4±3.2 ns.

We consider the K=1 level for the v=0 vibrational level. Miller and Freund[66] have calculated the zero field energy levels for K=1 and v=0,1,2,3. We have used these energy levels to calculate the approximate frequencies expected for the quantum beats of the hyperfine structure. These are given in Table I.

Now consider the time integral in Eq. (5.10):

$$\text{Int.} = \int_0^{t_1} \exp[-(\gamma+i\omega_{JF,J'F'})t]dt . \qquad (5.11)$$

Let

$$z = \gamma + i\omega_{JFJ'F'} , \tag{5.12}$$

so that Eq. (5.11) becomes

$$\text{Int.} = \int_0^{t_1} e^{-zt} dt = \frac{-e^{-zt_1}}{z} + \frac{1}{z} , \tag{5.13}$$

or,

$$\text{Int.} = \frac{-\exp[-(\gamma + i\omega_{JF,J'F'})t_1]}{\gamma + i\omega_{JFJ'F'}} + \frac{1}{\gamma + i\omega_{JFJ'F'}} \tag{5.14}$$

In an experiment, it is convenient to let t_1 be much longer than the lifetime of the state to increase the number of coincidences observed. Therefore if t_1 is much longer than either $1/\gamma$ or $1/\omega_{JFJ'F'}$, the first term on the right in Eq. (5.14) vanishes and we have

$$\text{Int.} \approx \frac{1}{\gamma + i\omega_{JFJ'F'}} . \tag{5.15}$$

From Table I, we can see that $\omega_{JFJ'F'}$ is typically on the order of 10^9 whenever $J \neq J'$ and $F \neq F'$, and vanishes otherwise. We can then approximate the integral by

$$\text{Int} \approx \begin{cases} 0 \text{ if } J \neq F' \text{ and } F \neq F' \\ \frac{1}{\gamma} \text{ if } J = J' \text{ or } F = F' \end{cases} \tag{5.16}$$

What happens physically in an experiment is that if $1/\omega_{JFJ'F'}$ is small compared to the lifetime and to the observation time, the photon intensity is "averaged out "over the quantum beats; and, if the lifetime of the state is short compared to the period of the quantum beats, only part of a cycle is completed before the molecule decays, and no

Table I. Expected Quantum Beat Frequencies for the $d^3\Pi_u$ (K=1) State of H_2.

J	J'	F	F'	$\omega_{JF,J'F'}$ (MHz)
0	0	1	1	0
0	1	1	0	1060
0	1	1	1	1514
0	1	1	2	1764
0	2	1	1	702
0	2	1	2	274
0	2	1	3	473
1	1	0	0	0
1	1	0	1	453
1	1	0	2	704
1	1	1	1	0
1	1	1	2	250
1	1	2	2	0
1	2	0	1	1764
1	2	0	2	1334
1	2	0	3	587
1	2	1	1	1816
1	2	1	2	1389
1	2	1	3	1041
1	2	2	1	2466
1	2	2	2	2038
1	2	2	3	1290
2	2	1	1	0
2	2	1	2	427
2	2	1	3	1175
2	2	2	2	0
2	2	3	2	748
2	2	3	3	0

effect is observed. Now using Eq. (5.16) for the time integral and Eq. (5.9) for the U's, we find for the process

$$e + X'\Sigma_g^+ \rightarrow d^3\Pi_u^- \ (K=1) + e' \ , \tag{5.17}$$

$$d^3\Pi_u^- \rightarrow a^3\Sigma_g^+(K=0) + h\nu$$

that the $A_{qq'}$'s are given by

$$A_{11} = [0.7126\ \sigma_1 + 0.295\ \sigma_0]\frac{1}{\gamma} \tag{5.18}$$

$$A_{00} = [0.5898\ \sigma_1 + 0.410\ \sigma_0]\frac{1}{\gamma} \tag{5.19}$$

$$A_{01} = [0.2442\langle f_0 f_1\rangle + 0.129\langle f_{-1} f_0\rangle]\frac{1}{\gamma} \tag{5.20}$$

$$A_{1-1} = [-0.1152\ \sigma_1]\frac{1}{\gamma} \tag{5.21}$$

The $^3\Pi_u^-$ rather than the $^3\Pi_u^+$ state was used because the dipole transition selection rules require $+\leftrightarrow-$, with $+\leftrightarrow+$ and $-\leftrightarrow-$. The singlet-to-triplet excitation by the electron does not violate our assumption that the scattering Hamiltonian has no spin dependent terms because the excitation above occurs via an electron exchange, rather than a spin flip. In the process described above, the measurement gives the excitation amplitude for the exchange process, and not a direct excitation.

B. Rotational Levels Not Resolved

Even when the rotational lines are not resolved, a measurement can yield some useful information about the scattering event. Two experimental aspects are involved:

the resolution of the incident electron beam; and the resolution of the detectors, particularly the resolution of the photon detector. First we consider the resolution of the electron beam. As discussed in Chapter II, the coherently excited states are those which can be expressed as a linear superposition, or, equivalently, those states which have the same dependence on the momentum vectors of the incident and scattered electrons. Where ΔE is the resolution of the beam, all states which have excitation energies within $\Delta E/2$ of the mean energy of the incident beam will be coherently excited. This implies that if ΔE is small enough that only a single K level of the molecule is excited (only the exactly degenerate magnetic substates are excited), the resolution of the detection apparatus doesn't matter. In practice this is not realizable, especially in the case of molecular targets, because several K levels of the ground state will be occupied, leading to differences in excitation energies for various K states that are much less than the rotational spacing. Resolutions on this order for electron guns are not now feasible.

We must assume then, that from a practical point of view, the electron beam will have a sufficiently large energy spread, ΔE, that several K levels will be excited. This means that the sum indicated in Eq. (5.1) should also include a sum over K:

$$|\Psi> = \sum_{KJM_J} f(KJM_K)|KJM_J \exp[-(\frac{\gamma}{2} + i\frac{E_{KJF}}{h})t] \qquad (5.22)$$

and a similar sum over K and K' in the equation for the $A_{qq'}$'s in Eq. (5.4). However, the natural widths of the K levels are small compared to the separation between the levels. The fact that the energy spacing between K and K' is large implies that $\omega_{KK'}$ is large, and we conclude by the same reasoning as in the preceding section that the time integral causes the terms in Eq. (5.4) to vanish if $K \neq K'$. This leaves only the sum over the unresolved K levels to be performed, and $A_{qq'}$ is now defined as

$$A_{qq'} \equiv \sum_{KJJ'FF'M_K M_K'} \left\{ U(qq'M_K M_K' JJ'FF'KK_{\mathcal{F}}) \langle f(KM_K') f(KM_K) \rangle \times \int_0^{t_1} \exp[-(\gamma + i\omega_{JFJ'F'})t]dt \right\} . \qquad (5.23)$$

The quantities U are defined in the same way as before. The sum over K has the same value as would be obtained if the K levels were incoherently excited.

The transitions most difficult to resolve are likely to be of the type*

$$K \to K_{\mathcal{F}}(=K-1) \text{ and } (K+1) \to K_{\mathcal{F}}(=K) . \qquad (5.24)$$

The energy difference between these transitions is much less than the separation between the levels K and K+1. Suppose, for example, that the apparatus could not resolve the transitions discussed in the case of $B'\Sigma_u^+ \to X'\Sigma_u^+$ where $K=1 \to K_{\mathcal{F}}=0$ and $K=2 \to K_{\mathcal{F}}=1$.

*See section C.2. of Chapter IV.

Using the notation σ_{KM_K} to label the differential cross sections for exciting the M_Kth sublevel of the K rotational state, the $A_{qq'}$ would now be given by

$$A_{00} = [\sigma_{10} + \frac{2}{3}\sigma_{20} + \sigma_{21}]\frac{1}{\gamma} , \tag{5.25}$$

$$A_{11} = [\sigma_{11} + \frac{1}{6}\sigma_{20} + \frac{1}{2}\sigma_{21} + \sigma_{22}]\frac{1}{\gamma} , \tag{5.26}$$

$$A_{01} = [\langle f(1,0)f(1,1)\rangle + \frac{\sqrt{3}}{3}\langle f(2,0)f(2,1)\rangle + \frac{\sqrt{3}}{6}\langle f(2,-1)f(2,0)\rangle]\frac{1}{\gamma} , \tag{5.27}$$

and

$$A_{1-1} = [-\frac{1}{2}\sigma_{11} + \frac{\sqrt{6}}{3}\mathrm{Re}\langle f(2,0)f(2,1)\rangle - \frac{1}{2}\sigma_{21}]\frac{1}{\gamma} . \tag{5.28}$$

C. Hund's Case (a) Coupling

In this section we consider the theory developed in the preceding chapters as applied to molecules obeying Hund's case (a) coupling. This coupling scheme is illustrated in Fig. 5.

In this coupling scheme, the orbital angular momentum is strongly coupled to the internuclear axis as in case (b) coupling with projection onto the internuclear axis Λ. The electronic spin is also strongly coupled to the internuclear axis with projection quantum number Σ. The total electronic angular momentum projection on the internuclear axis is Ω. The rotational angular momentum $\vec{N}$ is coupled

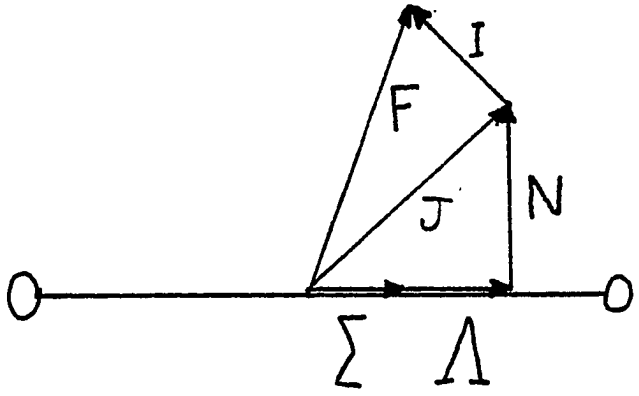

Fig. 5. Schematic diagram of Hund's Case (a) Coupling.

to Ω to form the total molecular angular momentum excluding nuclear spin, $\vec{J}$; and the total nuclear spin $\vec{I}$ is coupled to $\vec{J}$ to form the total molecular angular momentum $\vec{F}$.

Clearly there is no distinction between Hund's cases (a) and (b) for S=1; for Σ states, case (a) does not occur, since it is the magnetic field of the orbiting electrons which tend to couple S to the axis. This coupling requires that the spin-orbit portion of the Hamiltonian is larger than in case (b) coupling, so that our assumption of no significant spin-orbit interaction for the decay may need to be examined. However, for the lighter molecules this interaction should cause a splitting of no more than 1 or 2 cm^{-1}, which is not important.

We are considering Hund's case (a) coupling because it describes the coupling scheme in some light molecules. There are also cases which are intermediate between case (a) and case (b). For example, consider a molecule which obeys a case (a) coupling scheme. As the rotational level is increased, the rotational velocity may become comparable to the precessional velocity of $\vec{S}$ about the internuclear axis. This has the effect of uncoupling $\vec{S}$ from the internuclear axis. When this occurs, the angular momentum coupling might better be described by case (b) coupling. In addition to the selection rules for case (b) coupling we have, $\Delta\Sigma=0$, (corresponding to $\Delta S=0$ in case (b) coupling) for dipole transitions.

In what follows, we assume that the molecular state is adequately described by case (a) coupling, and that the J levels are resolved by the apparatus. Hyperfine interactions are included, and all other assumptions of Chapter III, section A are taken as valid. We now refer to J as the rotational quantum number. The excited state of the molecule is described by

$$|\psi(t)\rangle = \sum_{FM_F} f(JFM_F)|JFM_F\rangle \exp[-(\frac{\gamma}{2} + i\,\frac{E_{JF}}{\hbar})t] \qquad (5.29)$$

where the excitation occurs at t=0. Since I does not enter the decay process, we write this wavefunction and the excitation amplitude in an uncoupled representation:

$$|JFM_F\rangle = \sum_{M_J M_I} \langle JM_J IM_I|JIFM_F\rangle |JM_J IJ_I\rangle \ , \qquad (5.30)$$

and

$$f(JFM_F) = \sum_{M_J M_I} \langle JM_J IM_I|JIFM_F\rangle f(JM_J IM_I) \ . \qquad (5.31)$$

At this point we recognize that the form of these equations is the same as the corresponding equations in Chapter III. If we make the associations in Table II, we find

$$U(qq'M_J M_J' FF' J J_{\mathcal{F}}) = \frac{(2F'+1)(2F+1)(2J+1)}{(2I+1)}(-1)^{J_{\mathcal{F}}+M_J+q} \times \sum_{\chi\nu} (2\chi+1)(-1)^{\chi} \begin{Bmatrix} 1 & 1 & \chi \\ J & J & J_{\mathcal{F}} \end{Bmatrix} \begin{Bmatrix} J & J & \chi \\ F & F' & I \end{Bmatrix}^2 \begin{pmatrix} 1 & 1 & \chi \\ -q & q' & \nu \end{pmatrix} \begin{pmatrix} J & J & \chi \\ -M_K' & M_K & -\nu \end{pmatrix} \ , \qquad (5.32)$$

Table II. Association of Quantum Numbers in Hund's case (a) and Hund's case (b).

case (a)		case (b)
J, M_J	$\rightarrow$	K, M_K
I, M_I	$\rightarrow$	S, M_S
$J_{\mathcal{F}}, M_J$	$\rightarrow$	$K_{\mathcal{F}}, M_K$

and

$$A_{qq'} = \sum_{FF'M_JM_J'} U(qq'M_JM_J'FF')\langle f_{M_J'} f_{M_J}\rangle \int_0^{t_1} dt \exp[-(\gamma + i\omega_{F,F'})t] \; . \tag{5.33}$$

The coincidence rate is given by Eqs. (3.55) where $A_{qq'}$ is defined by Eq. (5.33) with

$$B = \frac{3\gamma'}{8\pi} v n_0 n_A \tag{5.34}$$

and

$$\gamma' = \frac{8\pi}{3} \frac{e^2 \omega^2}{hc^3} \frac{|\langle J||X^1||J_{\mathcal{F}}\rangle|^2}{(2J+1)} \; . \tag{5.35}$$

CHAPTER VI

BRIEF SUMMARY AND CONCLUSIONS

In this work we present formulas for the analysis of inelastic electron-diatomic molecule collisions in which the scattered electron and subsequent decay photon are detected in coincidence. We hope this work will prove useful in analyses of prospective and/or current experiments of this type.

Our results express the coincidence rate in terms of the complex excitation amplitudes for magnetic sublevels of rotational states of diatomic molecules, the angular correlation of scattered electrons and photons, and other measured parameters, such as the time-dependence of the radiation.

An important aspect of this work is in relating empirical results to the calculations of cross sections or density matrices. Experimental data may be analyzed with this theory to determine the partial differential cross sections for the magnetic sublevels, and, consequently the rotational state cross sections needed for many engineering and scientific applications. In addition, one can determine the phase relations between excitation amplitudes;

this provides additional information about the excited state wavefunctions. The fine and hyperfine structure of diatomic molecules can also be studied in some cases.

Although our discussion has assumed that the incident particle is an electron, the theory is easily generalized to include scattering by positrons, protons, or ions.

From our estimates of counting rate and photon resolution, we conclude that the angular correlation experiment involving H_2 is experimentally feasible, and we anticipate that calculations of the excitation amplitudes or density matrices as well as measurements of the coincidence rates will be forthcoming.

REFERENCES

1. R. E. Bell, Alpha, Beta, and Gamma Ray Spectroscopy (Ed. Siegbahn, North Holland, Amsterdam, 1966).
2. D. R. Hamilton, Phys. Rev. 58, 122 (1940).
3. L. C. Biedenharn and M. E. Rose, Rev. Mod. Phys. 25, 729 (1953).
4. A. Corney, Adv. Elect. and Elect. Phys. 29, 115 (1970).
5. M. R. C. McDowell, Comm. At. and Mol. Phys. 6, 1 (1976).
6. R. E. Imhoff and F. H. Read, Rep. Prog. Phys. 40, 1 (1977).
7. S. Heron, R. W. P. McWhirter, E. H. Rhoderick, Nature 174, 564 (1954).
8. S. Heron, R. W. P. McWhirter, and E. H. Rhoderick, Proc. Roy. Soc. (London) A234, 565 (1956).
9. R. E. Imhof and F. H. Read, Chem. Phys. Lett. 3, 652 (1969).
10. H. Ehrhardt, M. Schulz, T. Tekzat, and K. Willmann, Phys. Rev. Lett. 22, 89 (1969).
11. A. Pochat, D. Rozual, and J. Peresse, J. Physique 34, 701 (1973).
12. I. C. Percival and M. J. Seaton, Phil. Trans. Roy. Soc. London A251, 113 (1958).
13. G. C. M. King, A. Adams, and F. H. Read, J. Phys. B 5, L254 (1972).

14. J. Macek, Phys. Rev. Lett. 23, 1 (1969).

15. J. Macek, Phys. Rev. A1, 618 (1970).

16. J. Macek and D. H. Jaecks, Phys. Rev. A4, 2288 (1971).

17. J. Wykes, J. Phys. B 5, 1126 (1972).

18. V. L. Jacobs, J. Phys. B 5, 2257 (1972).

19. U. Fano and J. Macek, Rev. Mod. Phys. 45, 553 (1973).

20. U. Fano, Rev. Mod. Phys. 29, 74 (1957).

21. K. Blum and H. Kleinpoppen, J. Phys. B 8, 922 (1975).

22. K. Blum and H. Kleinpoppen, Int. J. Quant. Chem. Symp. 10, 231 (1976).

23. J. Eichler and W. Fritsch, J. Phys. B 9, 1477 (1976).

24. M. Eminyan, K. B. MacAdam, J. Slevin, and H. Kleinpoppen, Phys. Rev. Lett. 31, 576 (1973).

25. M. Eminyan, K. B. MacAdam, J. Slevin, and H. Kleinpoppen, J. Phys. B 7, 1519 (1974).

26. H. Arriola, P. J. O. Teubner, A. Ugbabe and E. Weigold, J. Phys. B 8, 1275 (1975).

27. J. Slevin and P. S. Farago, J. Phys. B 8, L407 (1975).

28. A. Ugbabe, P. J. O. Teubner, E. Weigold, and H. Arriola, J. Phys. B 10, 71 (1977).

29. V. C. Sutcliffe, G. N. Haddad, N. C. Steph, and D. E. Golden, Phys. Rev. A17, 100 (1978).

30. D. H. Madison and W. N. Shelton, Phys. Rev. A7, 499 (1973).

31. L. D. Thomas, Gy Csanak, H. S. Taylor and B. S. Yarlgadda, J. Phys. B 7, 1719 (1974).

32. M. R. Flannery and K. J. McCann, J. Phys. B 8, 1716 (1975).

33. D. H. Bransden and K. H. Winters, J. Phys. B 9, 1115 (1976).

34. T. Scott and M. R. C. McDowell, J. Phys. B 9, 2235 (1976).

35. R. E. Imhoff and F. H. Read, J. Phys. B 4, 1063 (1971).

36. A. J. Smith, F. H. Read and R. E. Imhoff, J. Phys. B 8, 2869 (1975).

37. C. Backx, M. Klewer, M. J. Van der Weil, Chem. Phys. Lett. 20, 100 (1973).

38. D. Cvejanovic, A. Adams, and G. C. King, J. Phys. B 11, 1653 (1978).

39. A. N. Jette and P. Cahill, Phys. Rev. 176, 186 (1968).

40. P. Baltayan and O. Nedelec, J. Phys. B 4, 1332 (1971).

41. N. Böse, J. Phys. B 11, L309 (1978).

42. N. Böse and F. Linder (1978), to be published.

43. K. Blum and H. Jakubowicz, J. Phys. B 11, 909 (1978).

44. A. P. Yutsis, I. B. Levinson, and V. V. Vanagas, Theory of Angular Momentum (N.S.F., Washington D.C., 1960).

45. A. S. Davydov, Quantum Mechanics, 2nd ed. (Pergamon Press, New York, 1976).

46. D. M. Brink and G. R. Satchler, Angular Momentum, 2nd ed. (Oxford University Press, London, 1968).

47. M. A. Morrison, T. L. Estle, and N. F. Lane, Quantum States of Atoms, Molecules and Solids (Prentice-Hall,

Englewood, New Jersey, 1976).

48. S. B. Elston, S. A. Lawton, and F. M. J. Pichanick, Phys. Rev. A10, 225 (1974).

49. A. Edmunds, Angular Momentum in Quantum Mechanics (Princeton University Press, Princeton, New Jersey, 1957).

50. G. Herzberg, Spectra of Diatomic Molecules, 2nd edition (Van Nostrand Reinhold Company, New York, 1950).

51. M. Rotenberg, R. Bivins, N. Metropolis, and J. K. Wooten, Jr., The 3j and 6j Symbols (Technology Press, M.I.T., Cambridge, Massachusetts, 1959).

52. B. Rosen, Spectroscopic Data Relative to Diatomic Molecules (Pergamon Press, New York, 1970).

53. W. A. Goddard III, D. L. Huestis, D. C. Cartwright, and S. Trajmar Chem. Phys. Lett. 11, 329 (1971).

54. D. C. Cartwright, S. Trajmar, W. Williams, and D. L. Huestis, Phys. Rev. Lett. 27, 704 (1971).

55. L. A. Kuznetsova, N. E. Huzmenka, Yu. Ya Kuzyakov, and Yu. A. Plastinin, Sov. Phys. Usp. 17, 405 (1974).

56. C. C. Lin, to be published.

57. M. Halmann and I. Laulicht, J. Chem. Phys. 44, 2398 (1966).

58. P. M. Dehmer and W. A. Chinka, J. Chem. Phys. 65, 2243 (1976).

59. P. Erman, Phys. Scr. 11, 65 (1975).

60. D. Ray and J. D. Carette, Can. J. Phys. 52, 1178 (1974).

61. H. J. Andra, Physica Scripta 9, 257 (1974).

62. O. Poulsen and J. L. Subtil, Phys. Rev. A8, 1181 (1973).

63. H. G. Berry, J. L. Subtil, E. H. Pinnington, H. J. Andra, W. Wittmann, and A. Gaupp, Phys. Rev. A7, 1609 (1973).

64. P. Cahill, J. Op. Soc. of Am. 59, 875 (1969).

65. R. S. Freund and T. A. Miller, J. Chem. Phys. 58, 3565 (1973).

66. T. A. Miller and R. S. Freund, J. Chem. Phys. 58, 2345 (1973).

APPENDIX I

DIAGRAMMATIC RECOUPLING

A. Symmetry Properties of 3j Coefficients.

In this appendix we define the symmetry properties of 3-j and 6-j Wigner coefficients and outline the basic operations of the diagrammatic technique[44] for reducing sums over products of CG coefficients.

The CG coefficient is related to the 3-j coefficient by

$$\langle j_1 m_1 j_2 m_2 | j_1 j_2 j_3 m_3 \rangle = (-1)^{j_1 - j_2 + j_3} (j_3)^{1/2} (-1)^{j_3 - m_3} \times$$

$$\times \begin{pmatrix} j_1 & j_2 & j_3 \\ m_1 & m_2 & -m_3 \end{pmatrix} , \qquad \text{(I-1)}$$

where

$$(j_3) \equiv 2j_3 + 1 . \qquad \text{(I-2)}$$

The 3-j coefficient is cyclically symmetric, i.e.,

$$\begin{pmatrix} j_1 & j_2 & j_3 \\ m_1 & m_2 & m_3 \end{pmatrix} = \begin{pmatrix} j_2 & j_3 & j_1 \\ m_2 & m_3 & m_1 \end{pmatrix} = \begin{pmatrix} j_3 & j_1 & j_2 \\ m_3 & m_1 & m_2 \end{pmatrix} , \qquad \text{(I-3)}$$

and is multiplied by the phase factor $(-1)^{j_1+j_2+j_3}$ upon interchange of any two columns. Changing the sign of all quantities in the second row multiplies the 3-j coefficient by the same phase factor.

In addition, there is a triangle relation between the angular momenta which we denote by $\Delta(j_1 j_2 j_3)$, which gives the useful inequality

$$j_1 + j_2 \geq j_3 \geq |j_1 - j_2| \ . \tag{I-4}$$

The projections obey the sum rule

$$m_1 + m_2 + m_3 = 0 \ . \tag{I-5}$$

These two relations imply

$$j_1 + j_2 + j_3 = \text{integer} \ . \tag{I-6}$$

A violation of (I-4), (I-5), or (I-6) results in a zero value for the 3-j coefficient.

B. Symmetry Properties of 6-j Coefficients.

The 6-j coefficient is expressed in terms of the 3-j coefficients as

$$\begin{Bmatrix} j_1 & j_2 & j_3 \\ \ell_1 & \ell_2 & \ell_3 \end{Bmatrix} = \sum_{\text{all } m_i, n_i} (-1)^{\sum_{\nu=1}^{3} (j_\nu - m_\nu + \ell_\nu - n_\nu)} \begin{pmatrix} j_1 & j_2 & j_3 \\ m_1 & m_2 & -m_3 \end{pmatrix} \times$$

$$\times \begin{pmatrix} j_1 & \ell_2 & \ell_3 \\ -m_1 & n_2 & n_3 \end{pmatrix} \begin{pmatrix} \ell_1 & \ell_2 & j_3 \\ n_1 & -n_2 & m_3 \end{pmatrix} \begin{pmatrix} \ell_1 & j_2 & \ell_3 \\ -n_1 & -m_2 & -n_3 \end{pmatrix} \ . \tag{I-7}$$

It is invariant to interchange of any two columns, or the interchange of any two angular moments in a row with the corresponding angular momenta in the other row.

C. Graphical Representation of 3j Coefficients

We represent the 3-j coefficient graphically by a node with three lines radiating from it. Each line represents one of the angular momenta, and has an arrow on it to indicate the sign of the z-component. An arrow directed away from the node denotes a positive sign and an arrow directed toward the node denotes a negative sign. A plus (+) sign near the node indicates a counterclockwise order in which the angular momenta are to be coupled and a minus (-) sign indicates a clockwise direction. For example, the four 3-j coefficients in Eq. (I-7) are represented graphically in Fig. 6.

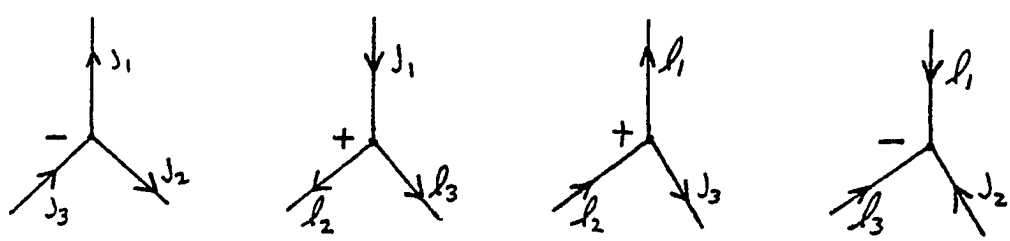

Fig. 6. Graphical Representation of 3j Coefficients.

The symmetry properties of these diagrams are quite simple: the lines may be deformed or rotated in any way we wish as long as the order of the coupling is not changed. If the

order of coupling is changed, a phase factor of $(-1)^{j_1+j_2+j_3}$ is introduced. Similarly, if the directions of all three arrows are changed, a phase factor of $(-1)^{j_1+j_2+j_3}$ results.

D. Contraction.

An angular momentum is said to be contracted when its projection is summed over. This operation can readily be performed graphically. First, the product of Wigner coefficients is put in a standard form. This form has two requirements:

i. The z-component to be summed over must appear twice in the product: once with a positive sign and once with a negative sign.

ii. Whenever a projection, m_j, is to be summed over, the terms in the sum must be multiplied by a factor $(-1)^{j-m_j}$.

The identity

$$(-1)^{j+m} = (-1)^{2j} \times (-1)^{j-m} \qquad \text{(I-8)}$$

is useful in reducing a sum to this form. As an illustration of the standard form, consider the right side of Eq. (I-7).

Graphically, contraction is carried out by joining the corresponding free lines of a particular angular momentum. (Free angular momenta are those not contracted.) Figure 7 shows a graphical contraction on j_1. Both arrows must have the same sense.

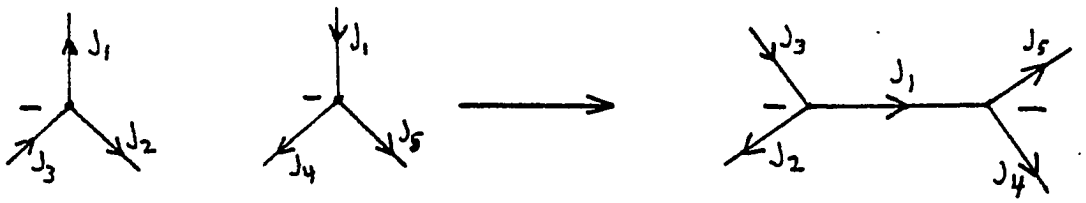

Fig. 7. Contraction on j_1.

E. Graphical Representation for a 6-j Coefficient.

The 6-j coefficient is defined by Eq. (I-7), which is in the standard form. When the graphical representations of the 3-j coefficients in this expression (Fig. 6) are contracted we obtain the diagram for the 6-j coefficient shown in Fig. 8.

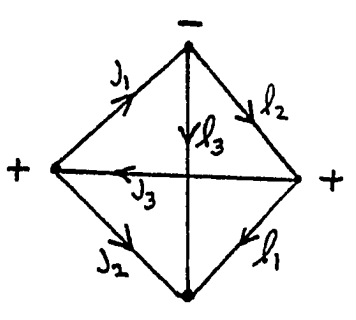

Fig. 8. Graphical Representation of 6-j Coefficient.

F. Expansion in Generalized Wigner Coefficients.

A generalized Wigner coefficient is a product of Wigner 3-j coefficients that have been minimally contracted. The result in Fig. 7 is an example of minimal contraction. Any general product of 3-j coefficients can be expanded as a product of "closed" figures (j-coefficients) multiplied by a generalized Wigner coefficient. This usually results in simplification of the original product. This procedure is detailed in Appendix II.A.

G. Separation of a Diagram.

It is sometimes desirable to break up a diagram. This can readily be accomplished if: (i) a line can be drawn through the diagram that crosses only three lines, and the separation is made on these lines; (ii) the three lines must have the same orientation. (The orientation of a closed (contracted) line, j, may be changed if a factor of $(-1)^{2j}$ is introduced.)

This separation is illustrated in Fig. 9.

We apply the results of this appendix to the simplification of complicated sums in Appendix II.

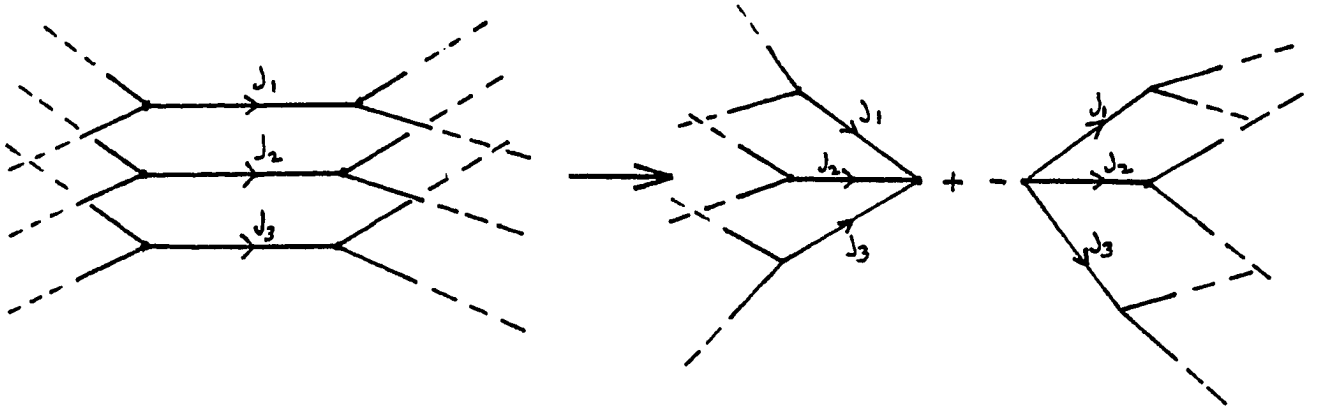

Fig. 9. Separation on three lines.

APPENDIX II

REDUCTION OF PRODUCTS OF SUMS OVER CLEBSCH-GORDAN COEFFICIENTS

In this appendix we apply the technique outlined in Appendix I to a product of six CG coefficients and to a product of ten CG coefficients.

A. Product of Six CG Coefficients.

We consider the sum

$$I = \sum_{\beta} \langle j_1 m_1 j_2 m_2 | j_3 m_3 \rangle \langle j_4 m_4 j_2 m_2 | j_5 m_5 \rangle \times$$
$$\times \langle j_{11} m_{11} j_6 m_6 | j_3 m_3 \rangle \langle j_7 m_7 j_6 m_6 | j_5 m_5 \rangle \times$$
$$\times \langle j_8 m_8 j_9 m_9 | j_1 m_1 \rangle \langle j_8 m_8 j_{10} m_{10} | j_4 m_4 \rangle \ , \qquad \text{(II-1)}$$

where

$$\beta \equiv \{m_1, m_2, m_3, m_4, m_5, m_6, m_8\} \ . \qquad \text{(II-2)}$$

Using Eq. (I-1) to change this sum over CG coefficients to a sum over 3-j coefficients gives

$$I = A \sum_{\beta} \begin{pmatrix} j_1 & j_2 & j_3 \\ m_1 & m_2 & -m_3 \end{pmatrix} \begin{pmatrix} j_4 & j_2 & j_5 \\ -m_4 & -m_2 & m_5 \end{pmatrix} \begin{pmatrix} j_{11} & j_6 & j_3 \\ -m_{11} & -m_6 & m_3 \end{pmatrix} \times$$
$$\begin{pmatrix} j_7 & j_6 & j_5 \\ -m_7 & -m_6 & m_5 \end{pmatrix} \begin{pmatrix} j_8 & j_9 & j_1 \\ m_8 & m_9 & -m_1 \end{pmatrix} \begin{pmatrix} j_8 & j_{10} & j_4 \\ -m_8 & -m_{10} & m_4 \end{pmatrix} (-1)^{P+R} \ , \qquad \text{(II-3)}$$

where

$$A \equiv [(j_3)^2(j_5)^2(j_1)(j_4)]^{1/2} , \qquad \text{(II-4)}$$

with

$$(j_i) \equiv (2j_i + 1) , \qquad \text{(I-2)}$$

and

$$R = j_1-m_1+j_2-m_2+j_3-m_3+j_4-m_4+j_5-m_5+j_6-m_6+j_8-m_8 , \qquad \text{(II-5)}$$

$$P = -m_7-m_9+j_7+2j_8-j_9 . \qquad \text{(II-6)}$$

The graphical representation for these 3-j coefficients are given in Fig. 10.

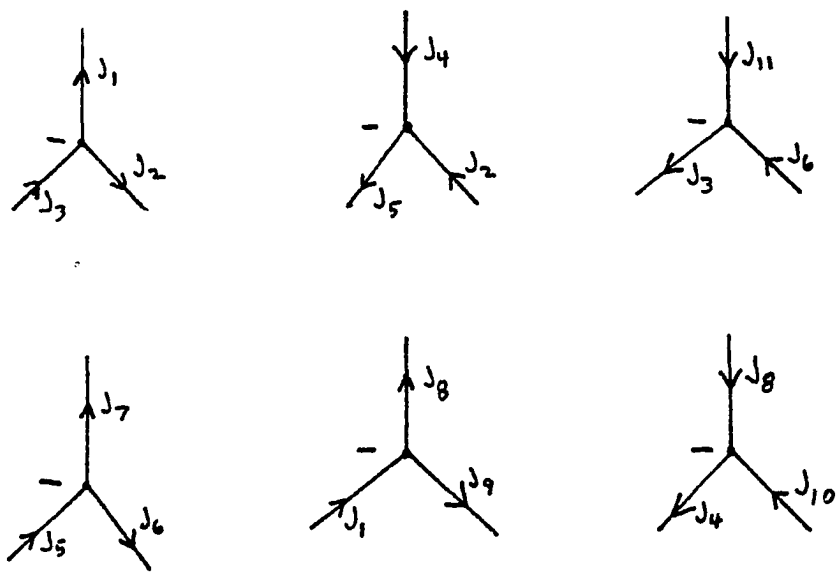

Fig. 10. Graphical Representation for Eq. (II-3).

Noting that R puts this expression into standard form, we contract on the indices β. This produces the diagram in Fig. 11.

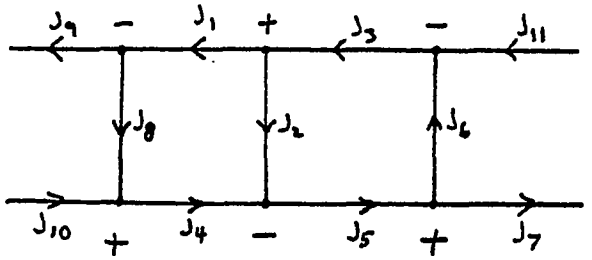

Fig. 11. Contraction of Eq. (II-3).

Contraction of this diagram with the generalized Wigner coefficient

$$\sum_{\nu} (2\chi+1)(-1)^{\chi-\nu} \begin{pmatrix} j_{10} & j_9 & \chi \\ -m_{10} & m_9 & \nu \end{pmatrix} \begin{pmatrix} j_{11} & j_7 & \chi \\ -m_{11} & m_7 & -\nu \end{pmatrix} , \qquad \text{(II-7)}$$

having a graphical representation shown in Fig. 12, results in the closed diagram of Fig. 13.

The diagram of Fig. (13b) is in the required form for separation along the dashed lines. We separate Fig. 13b as shown in Fig. 14.

Comparing these diagrams with the diagram for the 6-j coefficient in Fig. 8, we find that they represent the 6-j

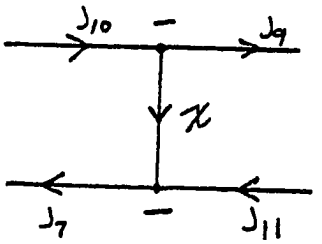

Fig. 12. Graphical representation of Eq. (II-7).

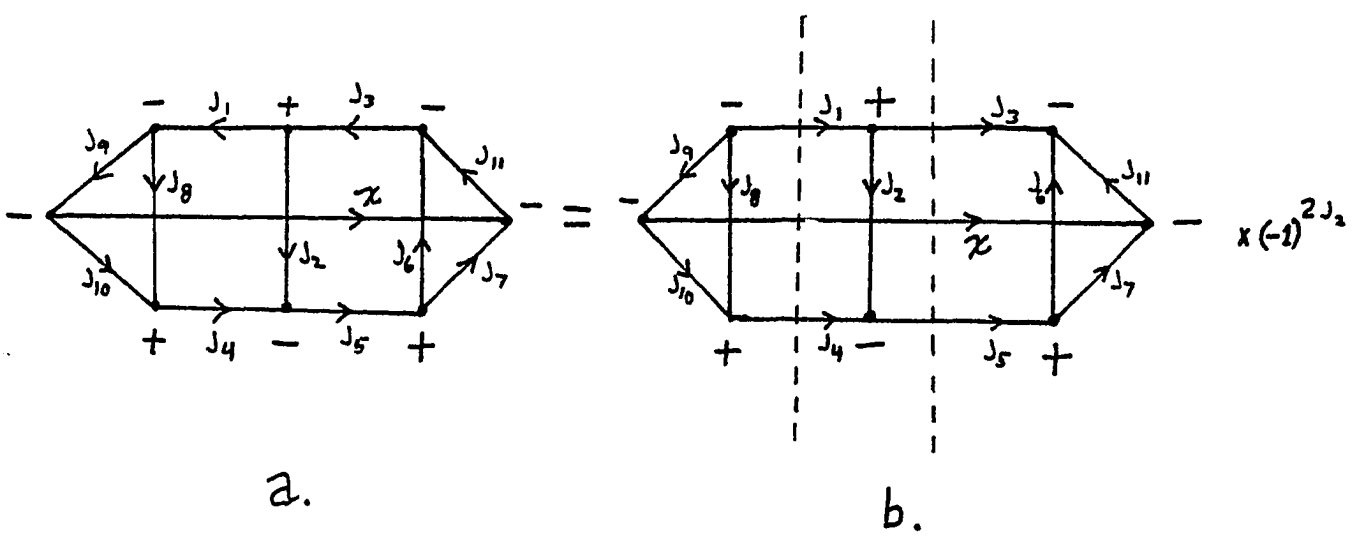

Fig. 13. Closed diagram for contraction of diagrams in Figs. (11) and (12).

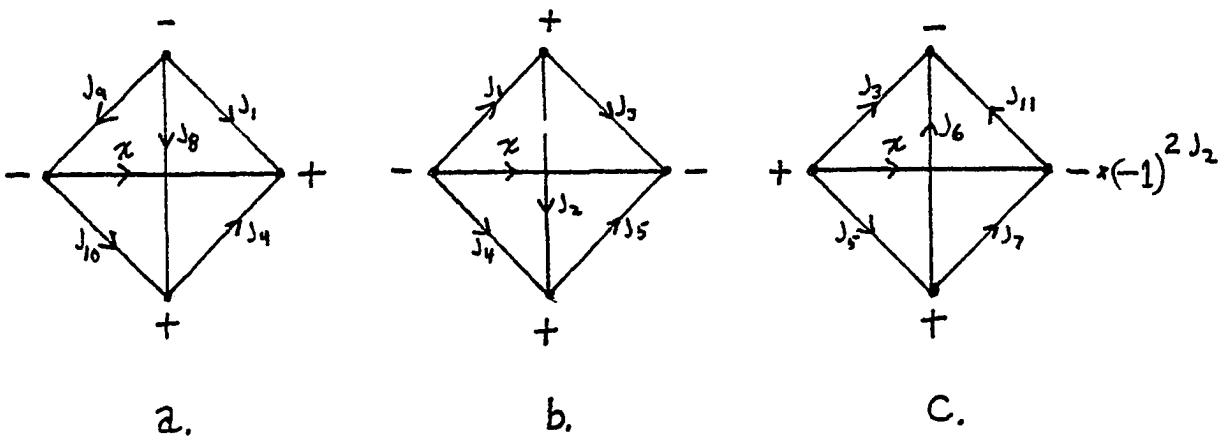

Fig. 14. Separation of diagram in Fig. 13.

coefficients:

$$\text{Fig. (14a):} \quad \begin{Bmatrix} j_9 & j_{10} & \chi \\ j_4 & j_1 & j_8 \end{Bmatrix} \times (-1)^{-j_4+j_8-j_9+2j_{10}-\chi} , \qquad \text{(II-8)}$$

$$\text{Fig. (14b):} \quad \begin{Bmatrix} j_1 & j_4 & \chi \\ j_5 & j_3 & j_2 \end{Bmatrix} \times (-1)^{-j_2+j_4-j_5} , \qquad \text{(II-9)}$$

and

$$\text{Fig. (14c):} \quad \begin{Bmatrix} j_3 & j_5 & \chi \\ j_7 & j_{11} & j_6 \end{Bmatrix} \times (-1)^{3\chi+j_5-j_6-j_{11}} . \qquad \text{(II-10)}$$

Combining these results we find

$$I = A(-1)^{P'} \sum_{\chi,\nu} (\chi)(-1)^{\chi-\nu} \begin{Bmatrix} j_9 & j_{10} & \chi \\ j_4 & j_1 & j_8 \end{Bmatrix} \begin{Bmatrix} j_1 & j_4 & \chi \\ j_5 & j_3 & j_2 \end{Bmatrix} \times$$

$$\times \begin{Bmatrix} j_3 & j_5 & \chi \\ j_7 & j_{11} & j_6 \end{Bmatrix} \begin{Bmatrix} j_{10} & j_9 & \chi \\ -m_{10} & j_9 & \nu \end{Bmatrix} \begin{Bmatrix} j_{11} & j_7 & \chi \\ -m_{11} & j_m & -\nu \end{Bmatrix} , \qquad \text{(II-11)}$$

where

$$P' = -m_7-m_9+j_2-j_6+j_7-j_8-2j_9+2j_{10}-j_{11} \cdot \qquad \text{(II-12)}$$

We associate the molecular angular momenta with these general quantities as

$$\begin{aligned} K &= j_1 = j_4 = j_7 = j_{11} & \bar{M}'_K &= m_1 \\ S &= j_2 = j_6 & \bar{M}_S &= m_2 \\ J' &= j_3 & M'_J &= m_3 \\ J &= j_5 & M_J &= m_5 \\ K_{\mathcal{H}} &= j_8 & \bar{M}_K &= m_4 \\ l &= j_9 = j_{10} & M_S &= m_6 \\ & & M_K &= m_7 \\ & & M_{K_{\mathcal{H}}} &= m_8 \\ & & q' &= m_9 \\ & & q &= m_{10} \\ & & M'_K &= m_{11} \cdot \end{aligned} \qquad \text{(II-13)}$$

The result is the reduction to Eq. (3.40).

B. Product of Ten Clebsch-Gordan Coefficients.

Consider the sum over products of CG coefficients:

$$\begin{aligned} I = \sum_{\beta} & \langle j_1 m_1 j_2 m_2 | j_3 m_3 \rangle \langle j_3 m_3 j_4 m_4 | j_5 m_5 \rangle \times \\ & \times \langle j_6 m_6 j_2 m_2 | j_7 m_7 \rangle \langle j_7 m_7 j_4 m_4 | j_8 m_8 \rangle \langle j_{16} m_{16} j_9 m_9 | j_{10} m_{10} \rangle \times \\ & \times \langle j_{10} m_{10} j_{11} m_{11} | j_5 m_5 \rangle \langle j_{12} m_{12} j_9 m_9 | j_{13} m_{13} \rangle \langle j_{13} m_{13} j_{11} m_{11} | j_8 m_8 \rangle \times \\ & \times \langle j_{14} m_{14} j_{15} m_{15} | j_{16} m_{16} \rangle \langle j_{14} m_{14} j_{17} m_{17} | j_{12} m_{12} \rangle , \end{aligned} \qquad \text{(II-14)}$$

where

$$\beta \equiv \{m_2, m_3, m_4, m_5, m_7, m_8, m_9, m_{10}, m_{11}, m_{12}, m_{13}, m_{14}, m_{16}\} . \quad \text{(II-15)}$$

Using Eq. (I-1) we write this equation in the standard form as

$$I = A \sum_{\beta} (-1)^{Q_1+Q_2} \begin{pmatrix} j_1 & j_2 & j_3 \\ m_1 & m_2 & -m_3 \end{pmatrix} \begin{pmatrix} j_3 & j_4 & j_5 \\ m_3 & m_4 & -m_5 \end{pmatrix} \begin{pmatrix} j_6 & j_2 & j_7 \\ -m_6 & -m_2 & m_7 \end{pmatrix}$$
$$\times \begin{pmatrix} j_7 & j_4 & j_8 \\ -m_7 & -m_4 & m_8 \end{pmatrix} \begin{pmatrix} j_{16} & j_9 & j_{10} \\ -m_{16} & -m_9 & m_{10} \end{pmatrix} \begin{pmatrix} j_{10} & j_{11} & j_5 \\ -m_{10} & -m_{11} & m_5 \end{pmatrix} \begin{pmatrix} j_{12} & j_9 & j_{13} \\ m_{12} & m_9 & -m_{13} \end{pmatrix}$$
$$\times \begin{pmatrix} j_{13} & j_{11} & j_8 \\ m_{13} & m_{11} & -m_8 \end{pmatrix} \begin{pmatrix} j_{14} & j_{15} & j_{16} \\ -m_{14} & -m_{15} & m_{16} \end{pmatrix} \begin{pmatrix} j_{14} & j_{17} & j_{12} \\ m_{14} & m_{17} & -m_{12} \end{pmatrix} \quad \text{(II-16)}$$

where $A = [(j_3)(j_5)^2(j_7)(j_8)^2(j_{10})(j_{13})(j_{16})(j_{12})]^{1/2}$, (II-17)

with

$$Q_1 = \sum_{i=2}^{16} (j_i - m_i) - j_6 + m_6 - j_{15} + m_{15} , \quad \text{(II-18)}$$

and

$$Q_2 = -m_1 - m_{17} - j_1 + 2j_4 + 2j_{11} + 2j_{14} + 2j_6 - j_{17} . \quad \text{(II-19)}$$

The graphical representation of these coefficients are given in Fig. 15.

These diagrams are contracted on the indicated indices, producing the diagram in Fig. 16. The contraction of this diagram with the generalized Wigner coefficient

$$\sum_{\nu} (2\chi+1)(-1)^{\chi-\nu} \begin{Bmatrix} j_6 & j_1 & \chi \\ -m_6 & m_1 & \nu \end{Bmatrix} \begin{Bmatrix} j_{15} & j_{17} & \chi \\ -m_{15} & m_{17} & -\nu \end{Bmatrix} , \quad \text{(II-20)}$$

(diagram in Fig. 16) is shown in Fig. 17.

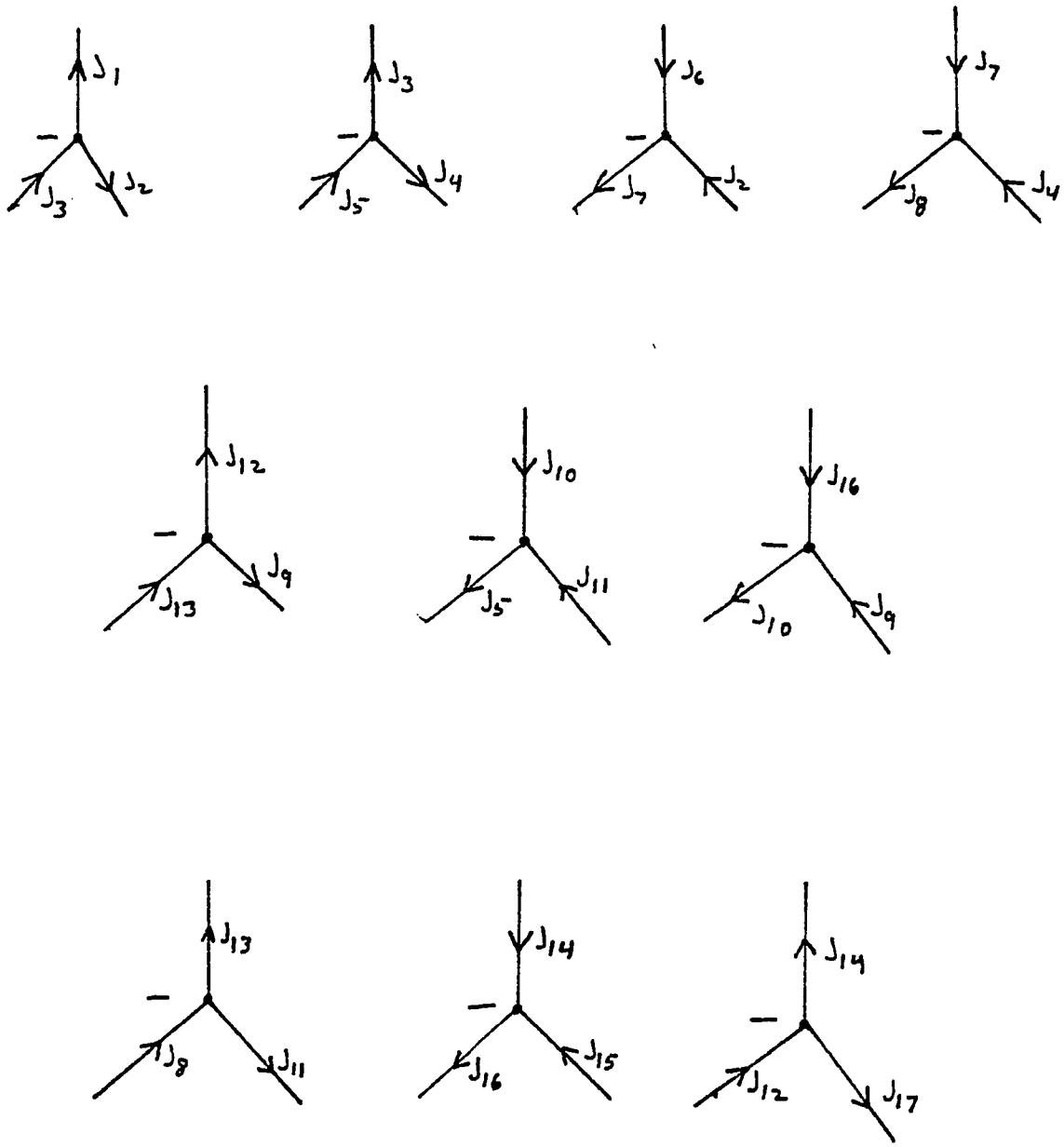

Fig. 15. Diagrams of ten 3-j coefficients.

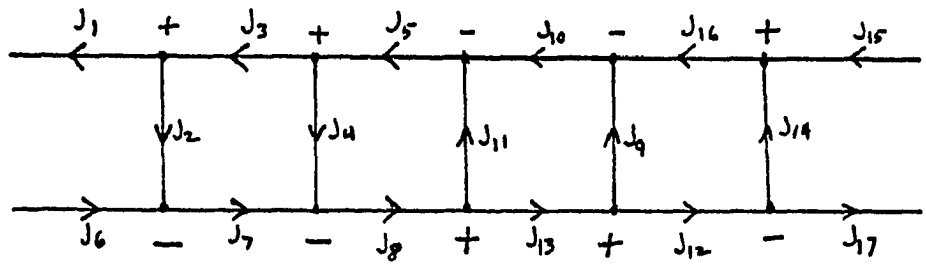

a.

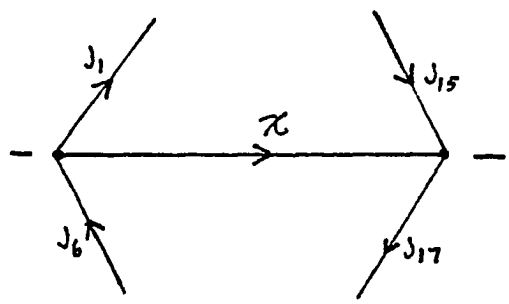

b.

Fig. 16. (a.) Contraction of ten 3-j coefficients.
(b.) Generalized Wigner coefficient that closes the jm-coefficient in (a.).

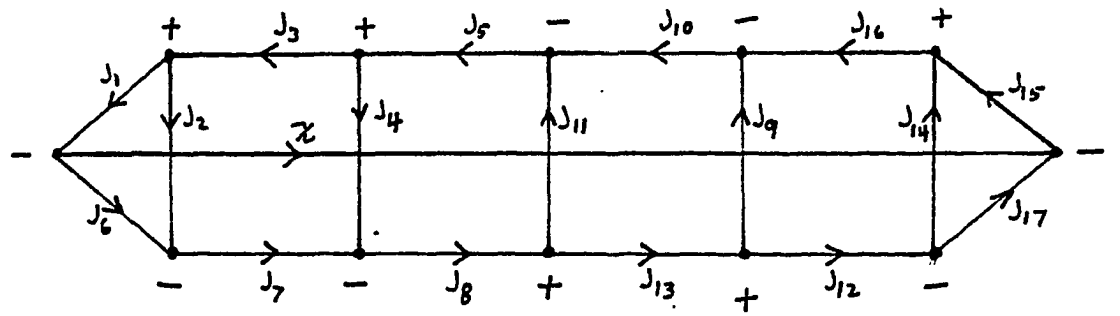

a.

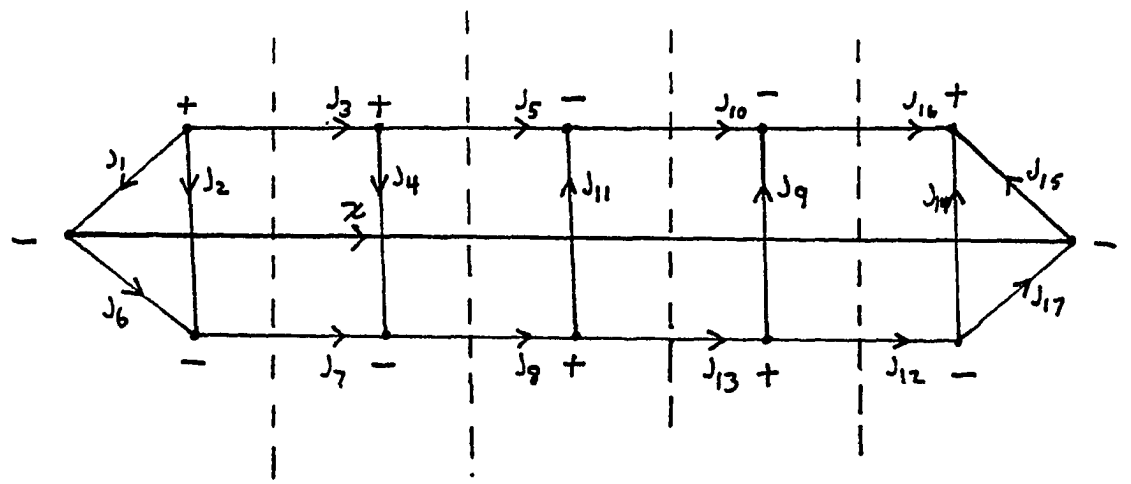

$$\kappa(-1)^{2J_3+2J_5+2J_{10}+2J_{16}}$$

b.

Fig. 17. (a.) Contraction of Figs. (16a) and (16b). (b.) Rearrangement to permit separation along the dashed lines.

This diagram is separated on the dashed lines in Fig. 17b. The result is shown in Fig. 18.

Comparing the diagrams of Fig. 18a-e, to the diagram of a 6-j coefficient, we find that they correspond, respectively, to

$$\begin{Bmatrix} j_1 & j_6 & \chi \\ j_7 & j_3 & j_2 \end{Bmatrix} (-1)^{2j_7-\chi+j_6+j_2+j_3} , \qquad \text{(II-21)}$$

$$\begin{Bmatrix} j_3 & j_7 & \chi \\ j_8 & j_5 & j_4 \end{Bmatrix} (-1)^{-j_8+2j_3+j_7+j_4+2j_5} , \qquad \text{(II-22)}$$

$$\begin{Bmatrix} j_5 & j_8 & \chi \\ j_{13} & j_{10} & j_{11} \end{Bmatrix} (-1)^{-j_{13}+2\chi-j_{11}+j_8} , \qquad \text{(II-23)}$$

$$\begin{Bmatrix} j_{10} & j_{13} & \chi \\ j_{12} & j_{16} & j_9 \end{Bmatrix} (-1)^{-j_{12}-\chi-j_9+2j_{13}+j_{10}} , \qquad \text{(II-24)}$$

and

$$\begin{Bmatrix} j_{16} & j_{12} & \chi \\ j_{17} & j_{15} & j_{14} \end{Bmatrix} (-1)^{-j_{17}-j_{14}+j_{12}+2j_{16}} . \qquad \text{(II-25)}$$

Combining these results we obtain

$$I = A(-1)^R \sum_{\chi\nu} (2\chi+1)(-1)^{\chi-\nu} \begin{Bmatrix} j_1 & j_6 & \chi \\ j_7 & j_3 & j_2 \end{Bmatrix} \begin{Bmatrix} j_3 & j_7 & \chi \\ j_8 & j_5 & j_4 \end{Bmatrix} \begin{Bmatrix} j_5 & j_8 & \chi \\ j_{13} & j_{10} & j_{11} \end{Bmatrix} \times$$

$$\times \begin{Bmatrix} j_{10} & j_{13} & \chi \\ j_{12} & j_{16} & j_9 \end{Bmatrix} \begin{Bmatrix} j_{16} & j_{12} & \chi \\ j_{17} & j_{15} & j_{14} \end{Bmatrix} \begin{pmatrix} j_6 & j_1 & \chi \\ -m_6 & m_1 & \nu \end{pmatrix} \begin{pmatrix} j_{15} & j_{17} & \chi \\ -m_{15} & m_{17} & -\nu \end{pmatrix} , \qquad \text{(II-26)}$$

where $R = -m_1-m_{17}-j_1-j_4-j_6-2j_{17}+j_{11}+j_{14}+j_3-j_{10}-j_7$

$$+j_2+j_{13}-j_9 . \qquad \text{(II-27)}$$

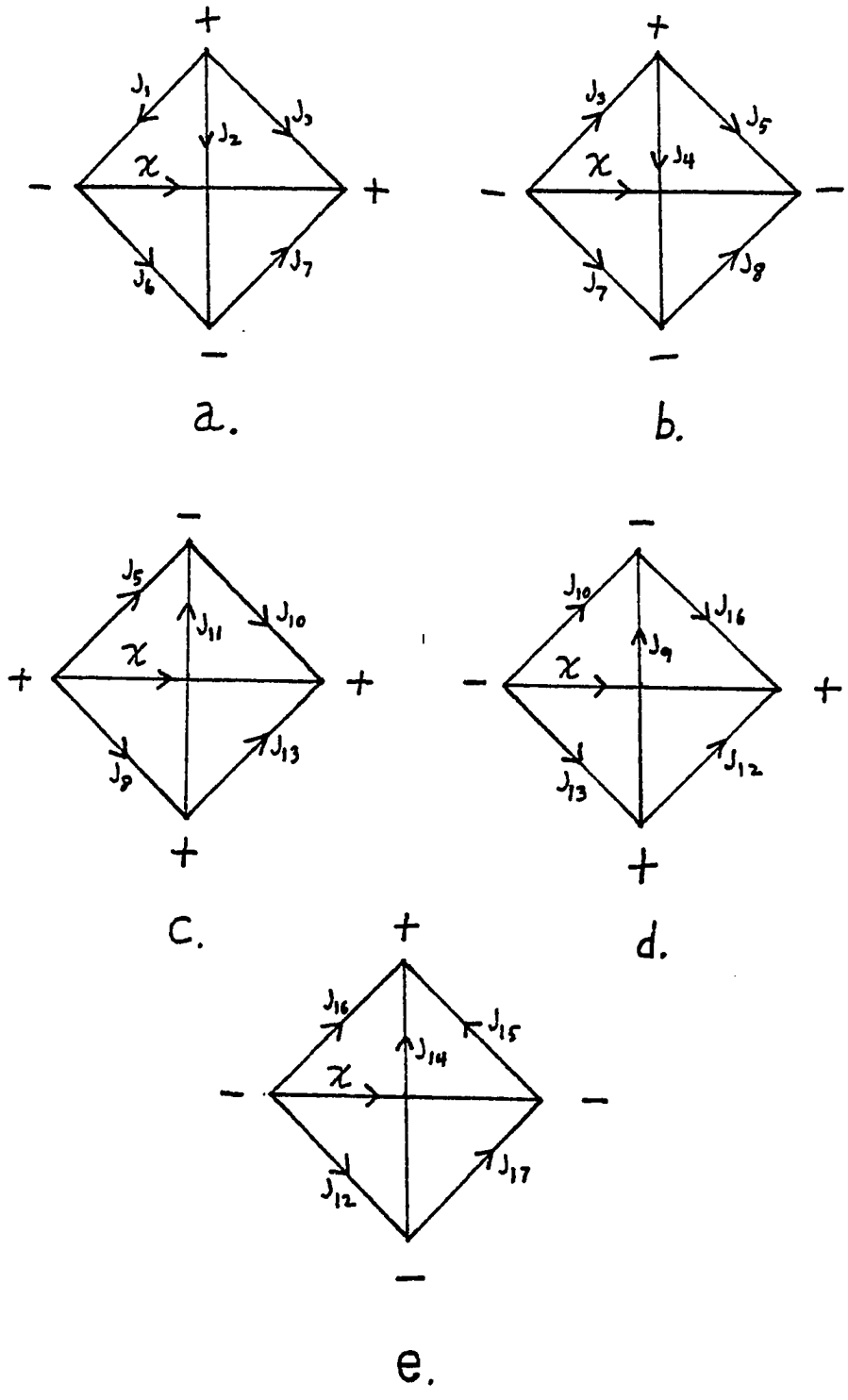

Fig. 18. Separation into 6-j coefficients.

We make the associations

$$
\begin{aligned}
S &= j_2 = j_9 & M'_K &= m_1 \\
J' &= j_3 = j_{10} & M_S &= m_2 \\
I &= j_4 = j_{11} & \overline{M}'_J &= m_3 \\
F' &= j_5 & M_I &= m_4 \\
J &= j_7 = j_{13} & M'_F &= m_5 \\
F &= j_8 & M_K &= m_6 \\
K_{\mathfrak{F}} &= j_{14} & \overline{M}_J &= m_7 \\
1 &= j_{15} = j_{17} & M_F &= m_8 \\
K &= j_1 = j_6 = j_{12} = j_{16} & M_{S_{\mathfrak{F}}} &= m_9 \\
& & M'_J &= m_{10} \\
& & M_{I_{\mathfrak{F}}} &= m_{11} \\
& & \overline{M}_K &= m_{12} \\
& & M_J &= m_{13} \\
& & M_{K_{\mathfrak{F}}} &= m_{14} \\
& & q' &= m_{15} \\
& & \overline{M}'_K &= m_{16} \\
& & q &= m_{17}
\end{aligned}
\qquad \text{(II-28)}
$$

to obtain Eq. (5.9).

APPENDIX III

The theory presented in this work involves many 3-j and 6-j coefficients. To facilitate their evaluation, we list in this appendix a computer program for this purpose. CG coefficients may be evaluated as well. The program is written in Basic computer language.

```
 4 GO TO 100
8 GO TO 1000
12 GO TO 1300
100 PRINT "THIS PROGRAM EVALUATES 6J-SYMBOLS"
110 DIM D(16),D1(16),Z1(7),Z2(7)
120 PRINT "INPUT THE 6J-SYMBOL, TOP ROW FIRST PLEASE"
130 INPUT J1,J2,J3,L1,L2,L3
140 D(1)=J1+J2-J3
150 D(2)=J1-J2+J3
160 D(3)=-J1+J2+J3
170 D(4)=J1+L2-L3
180 D(5)=J1-L2+L3
190 D(6)=-J1+L2+L3
200 D(7)=L1+J2-L3
210 D(8)=L1-J2+L3
220 D(9)=-L1+J2+L3
230 D(10)=L1+L2-J3
240 D(11)=L1-L2+J3
250 D(12)=-L1+L2+J3
260 D(13)=J1+J2+J3+1
270 D(14)=J1+L2+L3+1
280 D(15)=L1+J2+L3+1
290 D(16)=L1+L2+J3+1
300 FOR I=1 TO 16
310 IF D(I)<0 THEN 720
320 NEXT I
330 FOR I=1 TO 16
340 X=D(I)
350 GOSUB 660
360 D1(I)=X2
370 NEXT I
380 I2=J1+J2+J3+L1+L2+L3+1
390 W=0
400 FOR J8=1 TO I2
403 J=J8-1
410 Z1(1)=J-J1-J2-J3
420 Z1(2)=J-J1-L2-L3
430 Z1(3)=J-L1-J2-L3
440 Z1(4)=J-L1-L2-J3
450 Z1(5)=J1+J2+L1+L2-J
460 Z1(6)=J2+J3+L2+L3-J
470 Z1(7)=J3+J1+L3+L1-J
480 FOR I3=1 TO 7
490 IF Z1(I3)<0 THEN 600
500 NEXT I3
510 FOR I4=1 TO 7
520 X=Z1(I4)
530 GOSUB 660
540 Z2(I4)=X2
550 NEXT I4
```

```
560 X=J8
570 GOSUB 660
580 Z=Z2(1)*Z2(2)*Z2(3)*Z2(4)*Z2(5)*Z2(6)*Z2(7)
590 W=W+-1^J*(X2/Z)
600 NEXT J8
610 N=D1(1)*D1(2)*D1(3)*D1(4)*D1(5)*D1(6)*D1(7)*D1(8)*D1(9)*D1(10)
620 N=N*D1(11)*D1(12)/(D1(13)*D1(14)*D1(15)*D1(16))
630 S=W*SQR(N)
640 PRINT 'THE VALUE OF THE 6J-SYMBOL IS  ',S
650 END
660 X2=1
670 IF X=0 THEN 710
680 FOR I1=1 TO X
690 X2=I1*X2
700 NEXT I1
710 RETURN
720 PRINT 'THE VALUE OF THE 6J-SYMBOL IS ZERO!'
730 END
```

```
1000 QS=1
1010 PRINT "THIS PROGRAM EVALUATES WIGNER 3J-COEFFICIENTS"
1020 PRINT "INPUT THE ANGULAR MOMENTA FIRST, THEN THE PROJECTIONS"
1030 INPUT J1,J2,J3,M1,M2,M3
1040 IF M1+M2+M3=0 THEN 1065
1050 PRINT "THE VALUE OF THE 3J-SYMBOL IS ZERO"
1060 END
1065 DIM A(15),F(15)
1070 A(1)=J1+J2-J3
1080 A(2)=J1-J2+J3
1090 A(3)=-J1+J2+J3
1100 A(4)=J1+J2+J3+1
1110 A(5)=J1+M1
1120 A(6)=J1-M1
1130 A(7)=J2+M2
1140 A(8)=J2-M2
1150 A(9)=J3+M3
1160 A(10)=J3-M3
1170 FOR I=1 TO 10
1180 IF A(I)<0 THEN 1050
1190 X=A(I)
1200 GOSUB 660
1210 F(I)=X2
1220 NEXT I
1230 I2=2*(J1+J2)+1
1240 W=0
1250 FOR J=1 TO I2
1255 J6=J-1
1260 A(11)=J1+J2-J3-J6
1270 IF A(11)<0 THEN 1450
1280 A(12)=J1-M1-J6
1290 IF A(12)<0 THEN 1450
1300 A(13)=J2+M2-J6
1310 IF A(13)<0 THEN 1450
1320 A(14)=J3-J2+M1+J6
1330 IF A(14)<0 THEN 1450
1340 A(15)=J3-J1-M2+J6
1350 IF A(15)<0 THEN 1450
1360 FOR I5=11 TO 15
1370 X=A(I5)
1380 GOSUB 660
1390 F(I5)=X2
1400 NEXT I5
1410 X=J6
1420 GOSUB 660
1430 R=X2*F(11)*F(12)*F(13)*F(14)*F(15)
1440 W=W+-1^J6/R
1450 NEXT J
1460 S=SQR(F(1)*F(2)*F(3)*F(5)*F(6)*F(7)*F(8)*F(9)*F(10)/F(4))
1465 IF QS=0 THEN 1880
1470 V=-1^(J1-J2-M3)*S*W
1475 IF QS=0 THEN 1880
1480 PRINT "THE VALUE OF THE 3J-SYMBOL IS ",V
1490 END
```

```
1800 PRINT 'To evaluate Clebsch-Gordan coefficients, input the'
1810 PRINT 'ang. mom. first, then the projections in order'
1820 INPUT J1,J2,J3,M1,M2,M3
1830 M3=-M3
1840 Q5=0
1850 IF M1+M2+M3=0 THEN 1865
1860 PRINT 'THE CLEBSCH-GORDAN COEFFICIENT IS ZERO'
1870 END
1880 G2=2*J3+1
1881 V=S*W*SQR(G2)
1890 PRINT 'THE VALUE OF THE CLEBSCH-GORDAN COEF. IS',V
1900 END
```